DEVELOPMENT AND STUDY $CaO-B_2O_3-P_2O_5$ GLASS SYSTEM

A Thesis Submitted
In Partial Fulfillment of the Requirement
For the Degree of
M.Tech Dual Degree

By
Satendra Singh
ROLL NO. 710CR1174

DEPARTMENT OF CERAMIC ENGINEERING
NATIONAL INSTITUTE OF TECHNOLOGY
ROURKELA -769008
MAY 2015

DECLARATION

I am **Satendra Singh**, a student of Department of Ceramic Engineering, **National Institute of Technology Rourkela** bearing **Roll Number-710CR1174** hereby certify that my M.Tech Dual Degree Project Report entitled **" Development and study Cao-B_2O_3-P_2O_5 glass system"** under the guidance of Prof. Sumit Kumar Pal at National Institute of Technology, Rourkela. This is a record of bonafide work carried out by me and the results presented in the Project Report have not copied from any source. The results presented in this Project Record not have submitted to any other University or Institute for the award of any other certificate or degree.

Satendra

Rourkela
Date: 31/05/2015

Satendra Singh
Department Of Ceramic Engineering
National Institute of Technology
Rourkela-769008

CERTIFICATE

This is to certify that the thesis entitled**, "Development and study Cao-B_2O_3-P_2O_5 glass system"** Submitted by **Mr. Satendra Singh (710CR1174)** in partial Fulfillments for the requirements for the award of M.Tech Dual Degree in Ceramic Engineering at National Institute of Technology, Rourkela is an authentic work carried out by him under my supervision and guidance.

To the best of my knowledge, the matter embodied in this thesis has not been submitted to any other University/Institute for the award of any Degree or Diploma

Date:
01-06-2015

Supervisor:
Dr. Sumit Kumar Pal
Assistant Professor
Department of Ceramic Engineering
National Institute of Technology
Rourkela – 769008

ACKNOWLEDGEMENT

With deep respect, I avail this opportunity to express my gratitude to Dr. Sumit Kumar Pal, Assistant Professor, National Institute of Technology, Rourkela for his inspiration and guidance and valuable suggestion throughout this research work. It would have been impossible on my part to come out with this project report without him. I would like to express my gratitude to Dr. S. Pratihar (HOD), Ceramic Engineering for permitting to carry out my project. I would like to take this opportunity to thank all the faculty members of Ceramic engineering Department namely Dr. B.B. Nayak, Dr. Japes Bera, Dr. D. Sarkar, Dr. R. Sarkar, Mr. A. Choudhury, Dr. S. Behera, Dr. R. Mazumder, Dr. S. Das gupta, and Dr. S. Bhattacharyya. I would also take this opportunity to express my gratitude to the non-teaching staff Mr. Arvind Kumar, Mr. P.K Mohanty, Mr.Beheraand Mr. S.Sahoo. For their help and kind support, I would also like to thank Mr. Ezhil Venuswaran, Mr.Jayarao Gorinta, Mr.Satyananda Behera, Mr.KanchanMaji, Ms. Pinky Dey and Ms. Aiswarya Dash (PhD. Scholars) for the help and support in carrying out experiments and providing every sort of help possible. And last but not least, I am thankful to my friend Mr. Vikash Kumar Patel for his constant support and encouragement.

Satendra

Date:

Satendra Singh
Roll No. 710CR1174
Department of Ceramic Engineering
NIT Rourkela-769008

List of Tables

List of Figures

CONTENT

Page No.

Abstract

Glasses in the system 20wt%boric oxide and 80wt % [$CaO-P_2O_{5]}$ have been prepared by rapid quenching technic from the melts at high temperature. Ca/P molar ratios have been varied 1.65, 1.67 and 1.69. The amorphous nature of glass powder was confirmed by XRD analysis. Thermal and crystallization behavior were carried out by DSC analysis. The Sintering behavior and mechanical properties were investigated by dilatometry and biaxial flexural and diametral strength testing methods. The bioactivity of glass powder and glass scaffold were investigated after immersion in the simulated body fluid (SBF) for 1, 7, 14 &21 at 37.8^0c. Microstructural study has been analyzed using field emission scanning electron microscopy (FESEM). X-ray diffraction patterns clearly showed the deposition of Calium phosphate which is amorphous in nature.

CHAPTER: 1

INTRODUCTION

1.1 INTRODUCTION

Bio- materials that are implanted into bone defects are normally encapsulated by fibrous tissue separating them from the surrounding bone [1] .This is the normal behavior of the body towards inert materials. But ceramics, such as glass–ceramic A–W [2], Bio glass [3], and sintered hydroxyapatite [4] bond to living bone through bone-like apatite on their surfaces in the living body through this apatite layer. This ability of bonding of bone is called bioactivity. This bioactive glass and ceramics are previously used medically as important bone-bonding materials. Their ability of bone-bonding is supported by the formation of a biologically active apatite layer after reaction of the glass implant with the simulated body fluid [5, 6]. The bioactivity as well as biodegradability of a ceramic is controlled by the extent of surface reaction [7, 8]. At present, more emphasis is being given on silica free glass. High Ca/P molar ratio in silica free phosphate glasses makes them a promising candidate to be used as biomaterials because their chemical composition is matching closely with that of the natural bone [9]. Because of the high-temperature requirement and high crystallization tendency, these glasses are not easy to prepare. For example, preparation of borate base calcium phosphate glasses in the system with Ca/P molar ratio (1.65, 1.67, and 1.69) has been attained only by adding some amounts of other oxides. Moreover, boro-phosphate glasses have a variety of other useful properties such as zinc boro-phosphate glass have found applications as solder glasses [10], whereas many borophosphate glasses exhibited high chemical durability [11]. To my knowledge, there is not many research report on bioactivity of $CaO\text{-}P_2O_5\text{-}B_2O_3$ with Ca/P ratio 1.65,1.67 and 1.69 glass system. The main intension of this work was to development and study of 20 wt.%$[B_2O_3]$-80wt%$[CaO\text{-}P_2O_5]$ glass system with varying the Ca/P molar ratios (1.65, 1.67&1.69) and to investigate their mechanical and bioactive properties.

1.2 OBJECTIVE OF THE CURRENT PROJECT WORK

The prime objective of this project work is to development and study of **20 wt. % [B_2O_3]-80wt% [CaO-P_2O_5] glass system** with varying Ca/P molar ratios (1.65, 1.67&1.69).

The following points are aimed towards the fulfilling the objective of the present project work.

1. Preparation and characterization of glass powders
2. Study of thermal and crystallization kinetics of bioactive glasses
3. Study of sintering behavior and mechanical properties of bioactive glasses
4. Study of in vitro bioactivity tests comprised by the immersion of samples in SBF for different periods of time. .

CHAPTER: 2

LITRATUREREVIEW

Why Bio glass?

Bioactive glasses had been in demand as a bone substitution material due in recent health care industries due to their chemical stability, low density, and high wear resistance. [13, 16]. It had been widely accepted that scaffolds fabrication **[17]**. In another perspective, the dissolution rate of amorphous materials will be high when compared with crystalline material **[18].**The rate of dissolution of bio glasses will be more than the synthetic hydroxyapatite and other crystalline materials. This means, the regenerative capability of bioactive glasses is higher than not only with hydroxyapatite but also with other biomaterials. Bioactive glasses had been synthesized by the melt quench method and sol-gel method. Due to the mesoporous structure of sol gel derived glasses, they are highly bioactive than the melt quench glasses **[19]**.

Formation of Bioglass composition

Prof. L.L.Hench *et. al* had been driven by a hypothesis that the implant material along with calcium and phosphate materials would not be rejected by the human body unless it forms a Hydroxyapatite layer during in vivo analysis **[20]**. In order to confirm the hypothesis, ***L.L.Hench*** had formulated the 45S5 glass composition. By adapting the composition of Na_2O-SiO_2-CaO ternary system He had utilized (45 wt. % of SiO_2, 24.5 wt. % of Na_2O, 24.5 wt. % of CaO& 6 wt. % of P_2O_5) **[12].**Apart from this 45S5 glass composition, he had tested bioactivity on various other glass compositions.

Biocompatibility of bio glass

Prof. L.L.Hench et al had given the concept of bio incompatibility by his revolutionary 45S5 bioactive glass **[12]**.By which he had strong belief that it has the capability of bonding with the bone tissues. By cooperating with ***Dr. T.K.Greenlee***, he had conducted in vivo experiments on a

femoral model, which proved the bone bonding capability of 45S5 bioactive glass **[21]**. Furthermore they had ensured that this 45S5 bioactive glass composition has the capability of forming new bone tissue. By Invitro analysis, they had clearly confirmed the presence of carbonated hydroxyapatite phase on the surface of 45S5 bioactive glass. From this observation they had drafted a detailed Invitro mechanism of 45S5 bioactive glass in Simulated Body Fluid (SBF) **[22]**.Simulated Body Fluid (SBF) is an artificially synthesized body fluid which possesses the close ions present in the human body.

Production of Bioglass powder

The traditional approach of preparation of glass powders is the melt quench method. The first prepared bioglass powders are also carried out by melt quench method. While **L.L.Hench** was formulating the bioglass composition, he had included Na_2O in the 45S5 glass system to reduce the melting point of bioglass batch. As the 45S5 glass composition also fell close to the eutectic point, he was able to melt the glasses easily. The normal melting temperature of bio glasses will be around 1200°C to 1450°C. This temperature depends upon the alkali flux used in the glass system like Na_2O, K_2O and B_2O_3 etc. High quality phosphates, quartz or silica and carbonates are required for the preparation of melt derived glasses **[23]**.

Difference between the sole-gel glasses and melt quench glasses

The major differences acquired between sol-gel derived glasses and melt quench glasses are the surface area and porosity rate of the glasses, in general the textural properties **[24]**. Surface area of sol gel derived glasses will be high when compared to the melt quench glasses. Apparently the particle size of the melt derived glasses will be in micron range whereas in the case of sol gel glasses, it will be in the Nano range. These changes majorly influences the biological properties

by expecting higher ionic exchange with sol gel derived glasses than the melt derived glasses. Kinetically this leads to the rapid formation of a larger amount of apatite layer in sol-gel derived than the melt derived glasses. But the protocols of sol-gel derived glasses could not able to favor for bulk production. Thus by minimizing the synthesis errors and undergoing excessive milling, melt derived glasses had been used.

Why borate based bioactive glasses

Marta Giulia Cerrutietal The history of bioactive material leads to the improvement in preparation of such a bio glass which is inert and nontoxic to the human body. Glass former can be boron oxide and phosphorous pentoxide and the structure of glass is dependent on the glass modifier. Index of bioactivity can be calculated by using some mathematical formulae. Different techniques used to analysis the bioactive glass.

CHAPTER 3

EXPERIMENTALPROCEDURE

3.1 EXPERIMENTAL WORK

3.1.1 Bioactive glass composition and raw materials

The project started with the selection of the composition in the system of CaO-B_2O_3-P_2O_5 ternary bioactive glass composition. Had been carried out by keeping B_2O_3as 20 wt. % and 80 wt. % (CaO-P_2O_5) throughout the illustration. This had started to initiate the work by analyzing bioactive glass compositions with varying Ca/PMolar ratio (1.65, 1.67and1.69). The glass compositions selected in this current project work had been given in the table 3.1.1

BIOACTIVE GLASS	**B_2O_3 (In wt. %)**	CaO **(In wt. %)**	P_2O_5 **(In wt. %)**	Ca/P Molar ratio
Batch-1	20	45.27	34.72	1.65
Batch-2	20	45.50	34.49	1.67
Batch-3	20	45.74	34.25	1.69

Table 3.1– Bioactive glass compositions

The final raw materials used for the selected above glasses composition had been given in the table 3.2.

BIOACTIVE GLASS	**H_3BO_3 (wt. in gm)**	$CaCO_3$ **(wt. in gm)**	$(NH_4)_2HPO_4$ **(wt. in gm)**	Ca/P Molar ratio
Batch-1	35.52	80.80	64.61	1.65
Batch-2	35.52	81.22	64.17	1.67

Batch-3	35.52	81.64	63.74	1.69

Table 3.2 – Bioactive glass raw materials

Once the batch compositions (raw materials) are fixed, each batch was weighed stoichiometrically and mixed.

3.1.2 Determination of melting temperature

The temperature at which the materials are converted into the solid state to liquid state is known as the melting point of that materials. To find the melting temperature of the glass composition, first prepare a different batches named as batch-1, batch-2 and batch-3 with composition as mention in Table 3.2. After that three pellets were made for each glass composition through hydraulic pressing machine by using die-punch with a load 2 ton after that samples are dried in an oven at 60^0C. Then the pellets are placed into the furnace at different temperature (1300^0C, 1400^0C, 1500^0C) for 2 hours as soaking time. We observed that at 1300^0 C glass pellets just started to melt, at 1400^0 C glass pellets partial melting occurs, and at 1500^0 C the glass pellets completely convert into liquid state. So, finally the melting temperature was fixed to 1500^0 C for the above compositions.

3.1.3 Preparation of glass powder by melt quench method

After fixing the melting temperature as 1500^0C, without further processing, reagent grade H_3BO_3, $CaCO_3$ and $(NH_4)_2HPO_4$ were weighed as per the batch composition, and mixed homogeneously by using a mortar and pestle. The above-mentioned compositions were taken in three separate (Table 3.1.2) alumina crucibles and fired as per the optimized melting profile shown in Fig.3.1.2.

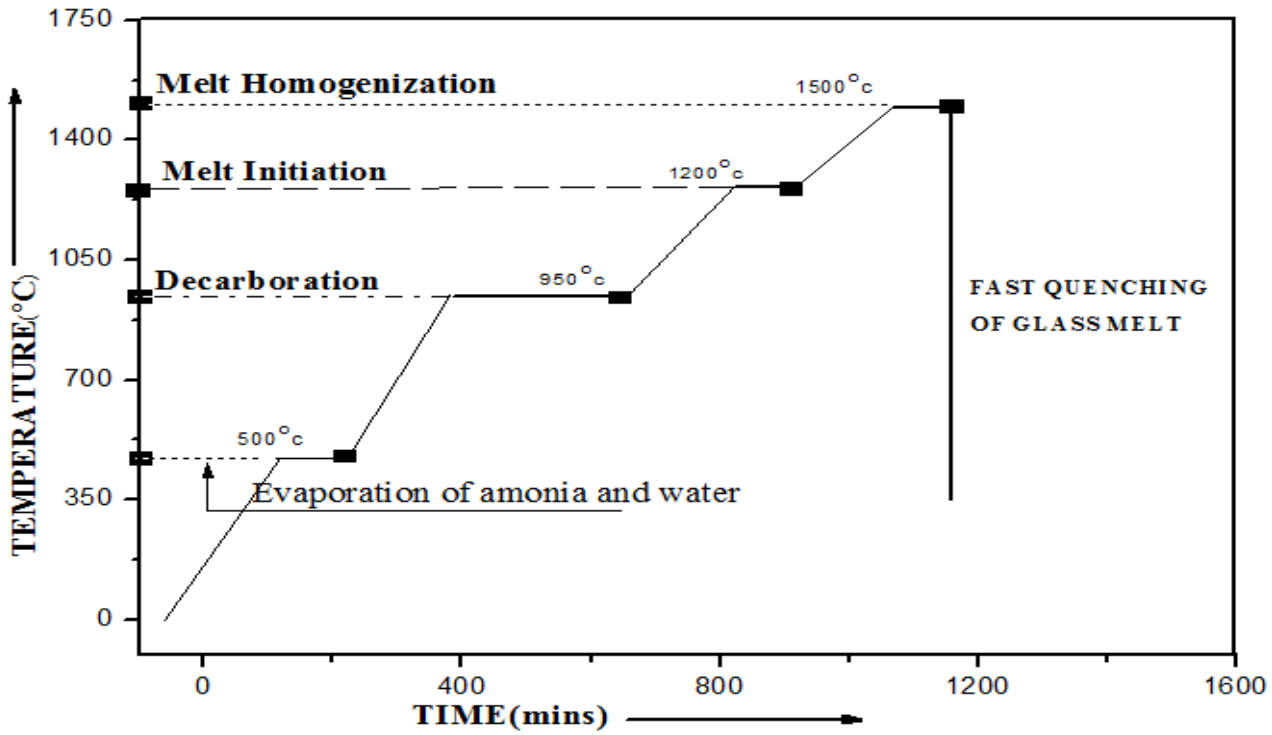

Fig 3.1– Melting profile of bioactive glasses

The glass melt was rapidly quenched in deionized water bath for the formation of glass frits. The milling of the glass frits was done for 6 hrs, at 350 rpm using planetary ball mill. The setup contains two silicon nitride jars with silicon nitride balls of diameter 20 mm (2 nos.) and 5 mm (13 nos.) the glass frits were wet milled using deionized water. After milling the slurry was dried in a hot air drier, then the loosely bonded agglomerates were grinded by hand using agate mortar and pestle.

Methodology of the glass powder preparation

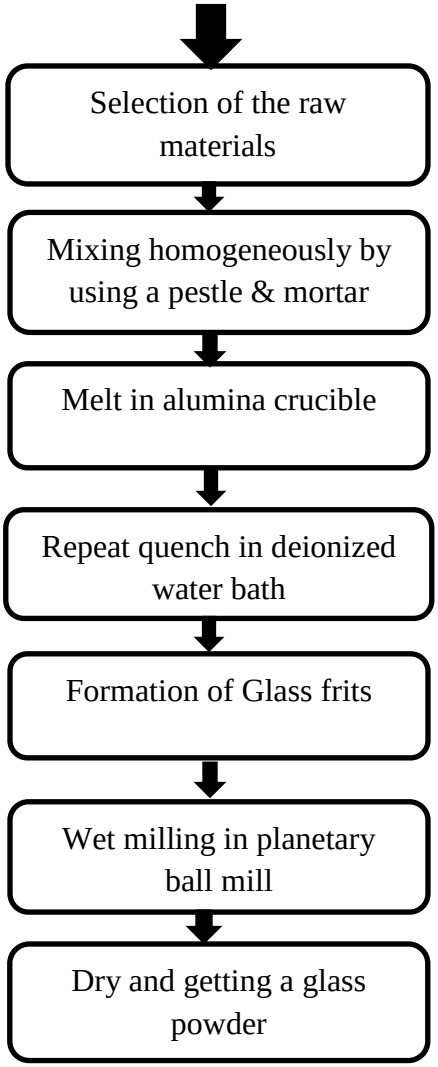

Fig. 3.2 methodology of the glass powder preparation

3.1.4 Fabrication of bioactive glass samples by uniaxial pressing

Porous bioactive glass sample had been prepared by using uniaxially pressed and sintering method. Naphthalene, had been used as a pore former. The bioactive glass powder (three batches Batch-1,Batch-2 and Batch-3) were mixed with different wt.% of naphthalene (0, 30 & 50 wt.%) and 3 wt.% PVA solution. The mixed powder was uniaxially pressed in a hydraulic press, at 221.6 MPa (3 US Tons) with dual time 90 sec, to form cylindrical pellets (13 mm Dia) and bar pellets with dimensions of the mold 60mm x5mmx5mm. The green samples were dried at around 70°C for 1 day in a hot air oven, for the decomposition of naphthalene. Then the samples were sintered at 1000^0C/2 h.

3.1.5 Sintering of the samples

Sintering of the glass pellets was done in an electric arc furnace. The sintering profile was as follows.

1.The first holding temperature was 300^0C/2h for complete removal of Naphthalene (boiling point 218^0C)

2. The second holding temperature was at 500^0C/2h for binder burn-out. PVA reduces by 90% at 400^0C.

3. The final holding temperature was at 1000^0C/2h for viscous sintering to take place.

4. The rate of heating maintained at 2^0C/min to avoid any defects in porous materials.

3.1.6 Invitro Analysis of samples by using SBF

The bioactive glass samples were immersed in the simulated body fluid (SBF) to analyze the regeneration capacity. The SBF was prepared by using a classical method. Kokubo et al. and many others invented a design for SBF concentration in such a way that they closely match with the ion concentrations present in the human blood plasma. Kokubo et al also confirmed the formation of apatite layer by immersing the bioglass in SBF. The aim of this experiment in this current project work is to see how the morphology of apatite layer had been differentiated between the porous and dense layer of porosity gradient samples. The relative composition depicts the close of ionic concentration of SBF with respect of human blood plasma design by Kokobu et al. shown in table 3.1.3

Ion	**Kukobo et al (mM)**	**Human Blood Plasma (mM)**
Na^+	142.0	142.0
Cl^-	147.8	103.3
HCO_3^-	34.2	27
K^+	5.0	5.0
Mg^{2+}	1.5	1.5
Ca^{2+}	2.5	2.5
HPO_4^{2-}	1.0	1.0
SO_4^{2-}	0.5	0.5

Table – 3.3 Illustration of ionic concentration of SBF and Human blood plas

The raw materials used and amount required for preparation of 1000ml of SBF shown in the table 3.4.

Order	Reagent	Amount (gpl)
1	NaCl	6.54
2	$NaHCO_3$	2.26
3	KCl	0.373
4	$Na2HPO_4.2H_2O$	0.17
5	$MgCl_2.6H_2O$	0.30
6	$CaCl_2.2H_2O$	0.36
7	Na_2SO_4	0.07
8	$(CH_2OH)_3CNH_2$	6.05

Table – 3.4 Raw materials used for preparation of SBF

1. The preparation of SBF was done in the 2000ml. Tarson Baker.
2. The selected chemicals had been added as per the sequence(as shown in table 3.4) in 700ml of deionised water.
3. The selected chemicals are not added unless the previous chemicals had been dissolved in the solution.
4. The 1M HCL had been added to adjust ph≈7.4 and ph measure using ph meter.and the temperature maintained 37^0c. throughout the process.
5. The solution was adjusted to 1000 ml by adding deionised water.
6. The solution transferred in a clean plastic bottle and keep at a temperature below 10^0c

Then the bioglass samples, which was sintered at 1000°C, had been kept in a 50ml polystyrene container. Almost 30ml of SBF had been poured into the container and kept for incubation. The bioactivity analysis had been carried out for 7,14 and 21 days. After incubation, the scaffolds had been dried at around 60°C. Furthermore, these scaffolds had undergone XRD and microstructural analysis to determine the Carbonated-hydroxyapatite formation.

3.2 CHARACTERIZATION WORK

3.2.1 Phase Analysis of bioactive glass powder by XRD

After preparation of the glass powder from the glass frits, the amorphous nature of the bioactive glass and the glass ceramic phases formed beyond the glass transition temperature had been investigated by using Philips X-ray Diffractometer with Ni-filter Cu-Ku (λ=1.5418 Å). The milled bioactive glass frits and make samples which had been compacted and sintered at 1000^0c. and make powder .had been kept for powder diffraction, The spectra were recorded between 10^0c to 80^0 c in 2θ continuous scanning modes, with step size 10^0/ minute. The operation voltage and current were 40 kV and 30 mA, respectively. Phase's identification was realized by comparing the experimental XRD patterns to standard inorganic crystal structure data (JCPDS).

3.2.2 DSC-Tg Analysis of bioactive glass powder

Thermal analysis of the bioactive glasses powder had been carried out by using DSC-TG analysis. Both differential scanning calorimetry and thermogravimetric analysis had been done with this equipment. DSC shows heat flow behavior of the samples. When the samples undergoes transformation, either absorbs energy or release energy. When absorb energy (endothermic) or release (exothermic) reactions. Similar, Thermo Gravimetric Analysis (TGA) is the study of mass change of a sample as a function of temperature. TG is useful for transformation involving absorption or release of gasses from the samples containing condensed phases. The DSC-TG experiment of the glass powder was done in a Netzsch STA/409c Thermal Analyzer. This instrument was done identify the temperature of different reaction take place.which can give us indication about the optimization of the crystallization, calcination temperature and etc.the glass powders was fired from room temperature to 900^0c in flowing

Argon environment. At a heating rate of 5^0/min,10^0/min and 15^0/min and the heat flow (mW/mg) and Mass loss(%) measurement was also observe with corresponding temperature in the same instrument and both the graphs were merged into one for comparative study.

3.2.3 Dilatometry Analysis of bioactive glass samples

Sintering and shrinkage behavior of the bioactive glass green compacts samples with 0 Wt. % Naphthalene had been studied by using Horizontal NETZSCH dilatometer model DIL 402C. The bar shaped pallet has been prepared with dimension (15mm x5mmx5mm) by using bioactive glass green compacts samples. Further, it undergoes respective characterization investigation. Sintering and shrinkage behavior of the bioactive glass green compacts samples had been observed by firing at room temperature up to 1000^0c with a heating rate of 10^0c/min, in an argon atmosphere.

3.2.4 Linear shrinkage analysis

The initial diameter had been measured for the green body after uniaxial pressing is done, and the final diameter had been measured for the sintered samples at 1000^0 c for 2hours.The linear shrinkage(%) of the sintered samples can be found by using the formula.

Linear Shrinkage = [(initial diameter-final diameter)*100/initial diameter] %

3.2.5 Bulk density and apparent porosity measurement

Bulk density and apparent porosity of the sintered samples had been determined by using Archimedes principle. After the sample had been prepared, the dry weight of the sample had been measured **(W_d)**. Then they had been immersed in kerosene and evacuated using a vacuum pump and desiccator till air bubbles stopped coming out (approximate 2 hours). This makes the kerosene get penetrated into the pores. Then soaked weight **(W_s)** and suspended weight**(W_a)** of the sample had been measured. Finally, the apparent porosity and bulk density of the samples had been measured by using the formulae as follows:

$$\textbf{Bulk density, } (B.D) = \left(\frac{W_d}{W_s - W_a}\right) * \textbf{Density of kerosene}$$

$$\textbf{Apparent porosity, } (A.P) = \left(\frac{W_s - W_d}{W_s - W_a}\right) * 100\%$$

3.2.6 Diametral tensile strength measurement of bioactive samples

Generally, diametral tensile strength is a mechanical property used to evaluate the performance of brittle materials under tensile stress. The samples that had been sintered at 1000°C had undergone diametral tensile strength measurement. The Diametric tensile strength had been calculated by using the formula

$$\textbf{\textit{Diametral tensile strength}} = \frac{2P}{\pi Dt}\ (MPa)$$

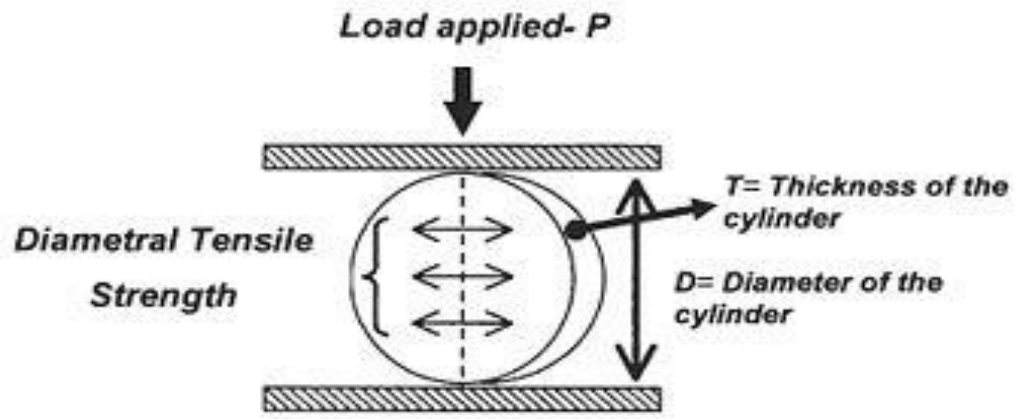

Fig.3.3- schematic illustration of diametral tensile strength measurement

3.2.7 Three-point bending moment measurement

Three-point bending or flexural strength is also known as Modulus of Rupture; it is a mechanical property for measuring the strength of the material. It is describes a material's ability to resist deformation under load. The samples without pore former and pore former of (60mm x6mm x6mm) size had been compacted at 3ton pressure and sintered at 1000°C. With a span of 40mm, the uniaxial loading had been given to the samples on 3point bending moment setup as shown in the Fig – 3.2.2.

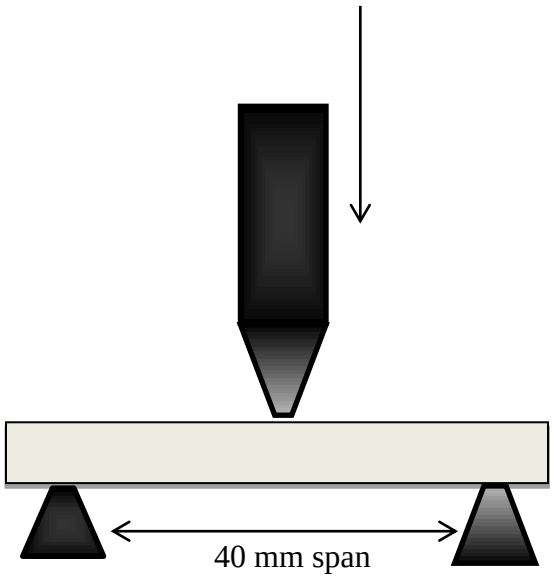

Fig – 3.4 Three points bending moment of dense bioactive glass

The desired glass samples placed it on the bearing edges of the machine and then start apply uniformly rate load at middle of the sample after that the load on which the sample breaks is noted and flexural strength of the sample. The flexural strength of the samples had been calculated by using the formula,

$$Flexural\ Strength,\ \sigma = \left(\frac{3FL}{2bd^2}\right)$$

Where

F– Applied load (N)

L – Distance between two bearing edges (mm)

b – Width of the sample (mm)

d – Thickness of sample (mm).

3.2.8 Vickers hardness measurement

Hardness is all shown the property of a material that resistance to the plastic deformation, by penetration. Hardness may also refer to resistance to bending, rubbing, scratch or cutting. In Vickers hardness test method, the test material is indented with a diamond indenter, in the form of a right pyramid with a square base and an angle of 136 degrees between opposite faces and a load of 3 Kgf was applied. The load was applied for 10 seconds. The two diagonals of the indentation in the surface of the material after removal of the load are measured with a microscope attached to the testing machine, and their average is calculated. The area of the indentation is calculated. The Vickers hardness is obtained by dividing the kgf load by the square mm area of the indentation. The indentation of the samples had been calculated by using the formula

$$HV = \frac{2.854F}{Area\ of\ indentation(d^2)}\ (MPa)$$

Where,

F=load

d= average of indentation

3.2.9 Scanning Electron Microscopy (SEM)

Microstructure of the HCA covered pellets immersed in SBF for 7days, 14days and 21 days were seen under SEM (JOEL-JSM 6480LV) using back scattered electron mode to study the growth of HCA with time, so as to verify the bioactivity the bioactivity of the material. The generator voltage was set at 15kv and the magnification war 200X. The pellets were washed in isopropyl alcohol. The samples were electroplated with platinum for making the surface conducting

CHAPTER 4

RESULTS AND DISCUSSION

4.1 Phase Analysis of bioactive glass powder

4.1.1 XRD Analysis of glass powder

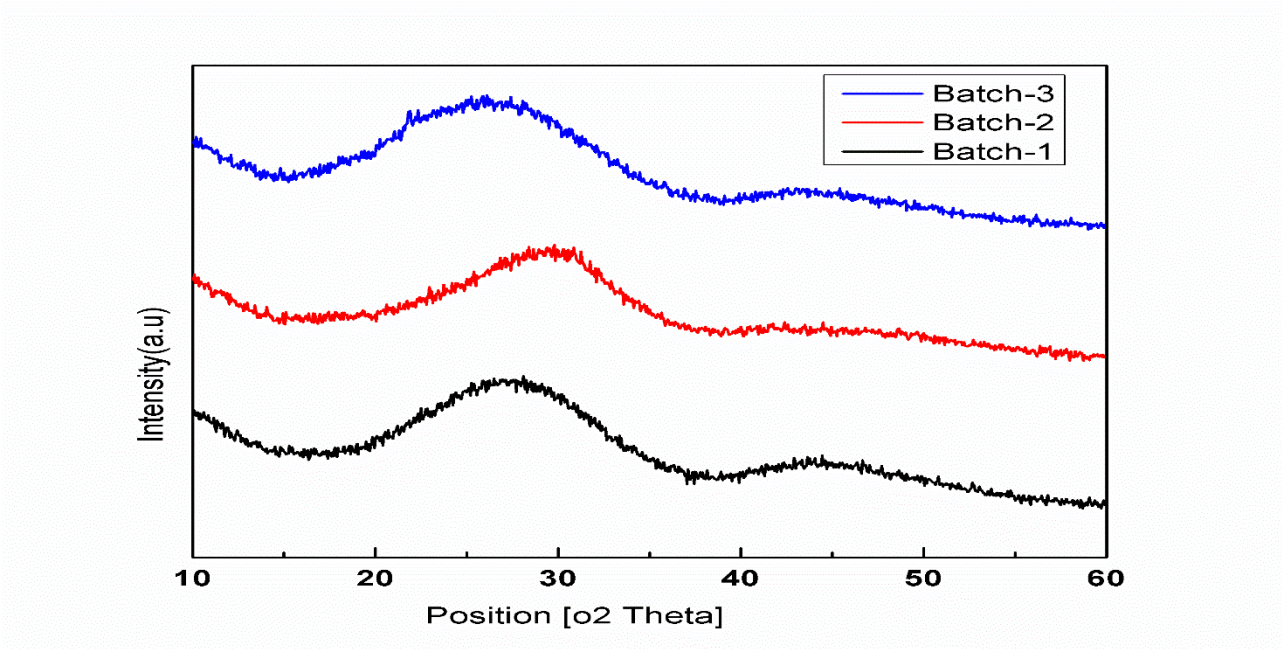

Fig.4.1 Powder X-ray diffraction pattern for glasses

XRD traces for the glass samples are presented in Figure (4.1) where a single broad peak between 20° and 35° was observed for each composition. The absence of any sharp crystalline peaks confirmed that all the glasses produced were amorphous.

4.1.2 XRD Analysis of sintered glass SBF samples

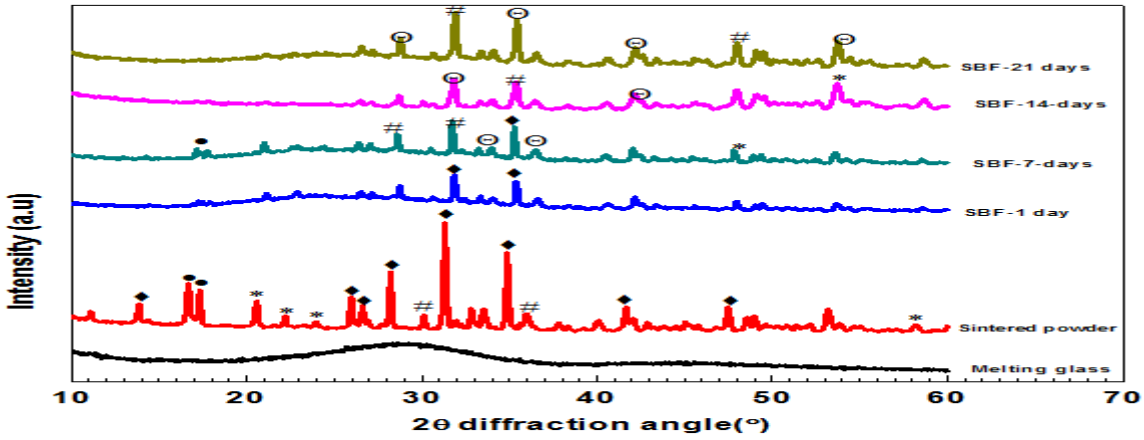

Figure 4.2 X-ray pattern Batch-1 of melting glass powder, sintered power, SBF-1 days, SBF-7 days, SBF-14-days, and SBF-21 days samples and their phases and reference code mention in table(4.1)

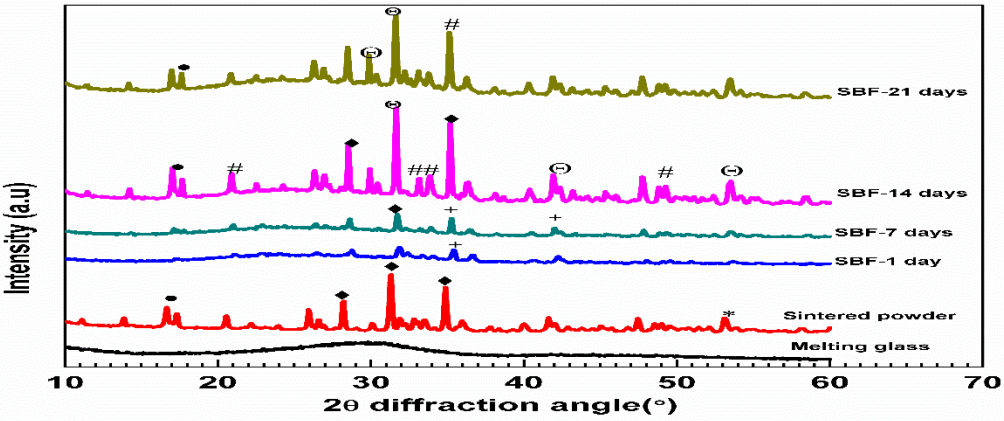

Figure 4.3 X-ray pattern batch-2 of melting glass powder, sintered power, SBF-1 days, SBF-7 days, SBF-14-days, and SBF-21 day's samples and their phases and reference code mention in table (4.1)

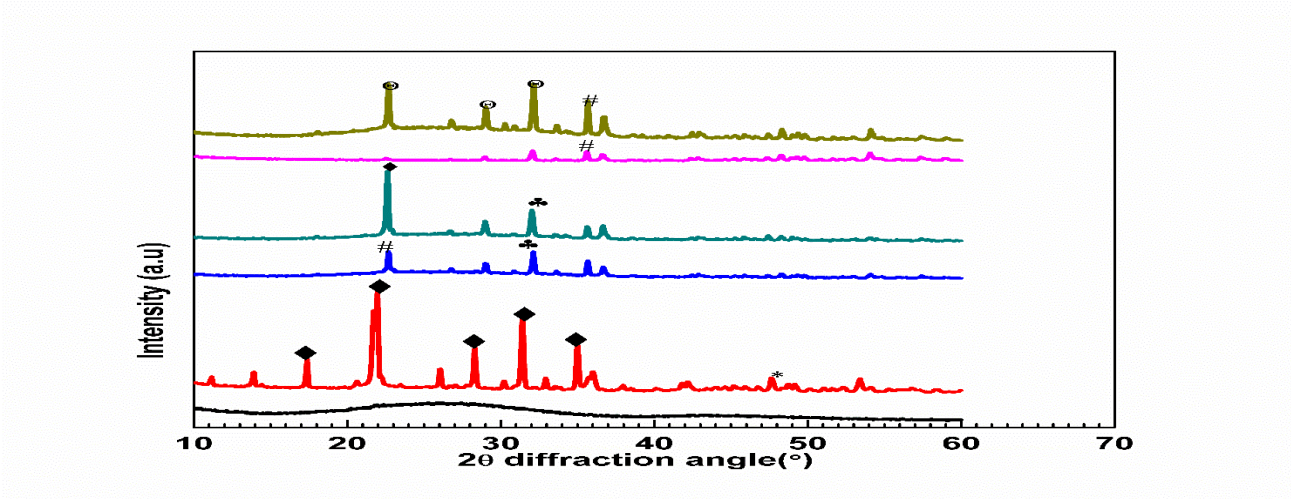

Figure 4.4 X-ray pattern batch-3 of melting glass powder, sintered power, SBF-1 days, SBF-7 days, SBF-14-days, and SBF-21 day's samples and their phases and reference code mention in table (4.1)

Symbols	Phases form	JCPDF References codes
♦	β-Ca_3 (PO4)$_2$	09-0169
*	$Ca_2B_2O_5$	22-0139
●	P_2O_5	83-0602
#	CaP_2O_6	15-0204
Θ	Ca_5 (PO_4)$_3$ (OH)	73-1731
♣	$CaPO_3$(OH)	09-0080

Table (4.1) XRD analysis phases and reference code

4.1.3 XRD Analysis of the of porous samples

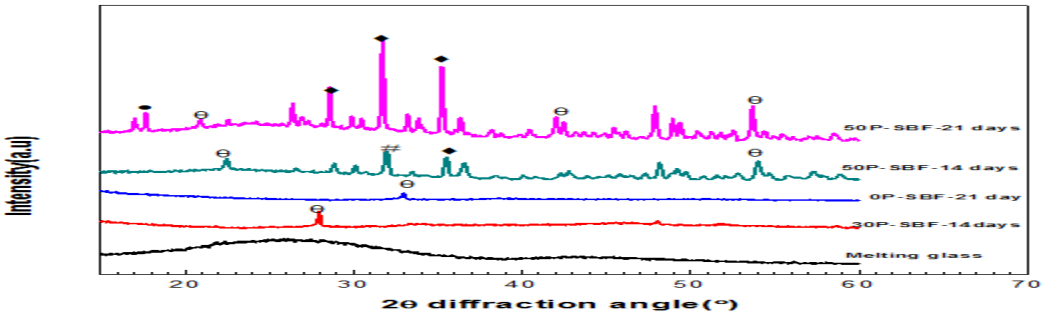

Figure 4.5 X-ray pattern batch-2 30p, 50p samples and their phases and reference code mention in table (4.2)

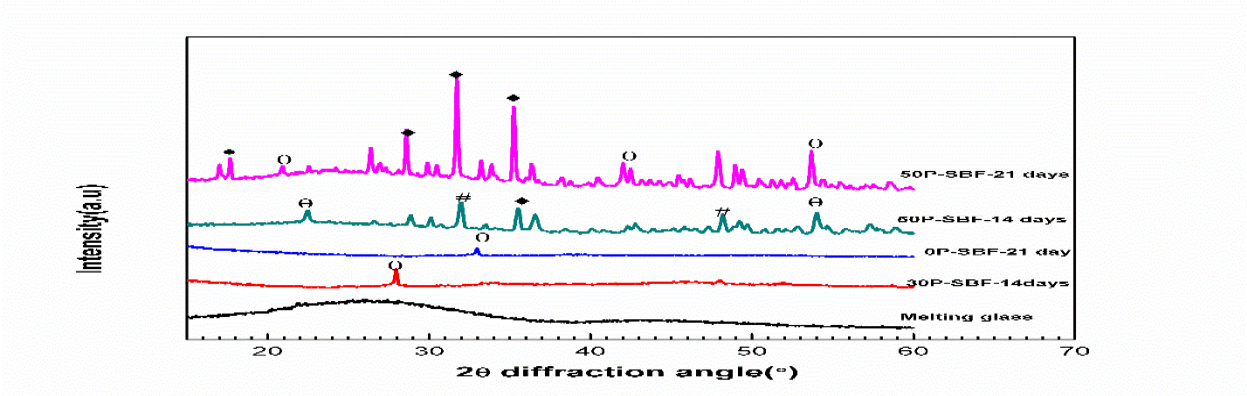

Figure4.6 X-ray pattern batch-3 30p, 50p samples and their phases and reference code mention in table (4.2)

Symbols	Phases form	References
♦	β-Ca3 (PO4)2	09-0169
●	P2O5	83-0602
Θ	Ca5 (PO4)3 (OH)	73-1731
#	CaP2O6	15-0204

Table (4.2) XRD analysis phases and reference code

4.1.4 XRD analysis of the powder SBF samples

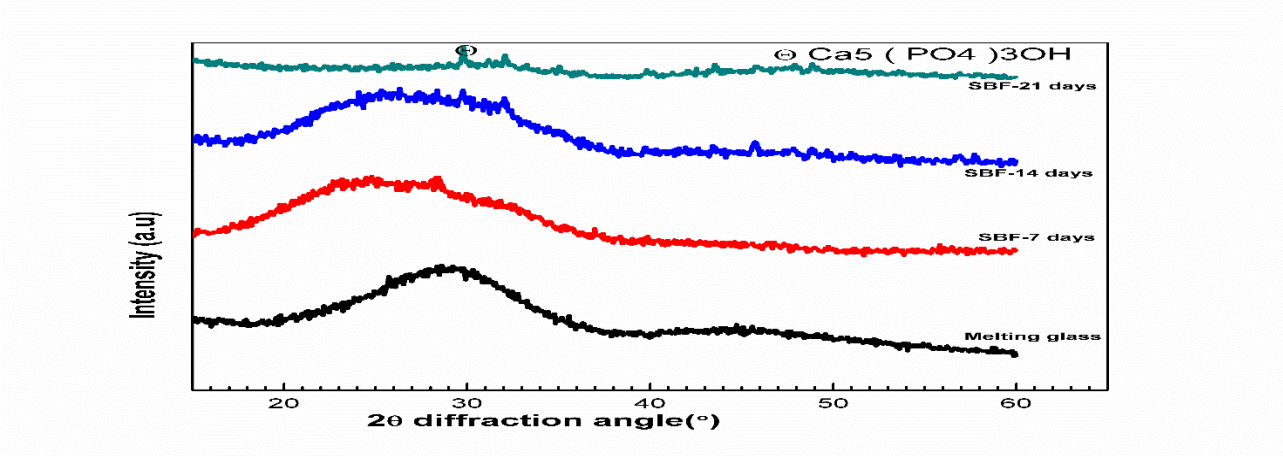

Figure4.7 X-ray pattern batch-1 glass powder SBF samples and their phases with reference code mention in table (4.3)

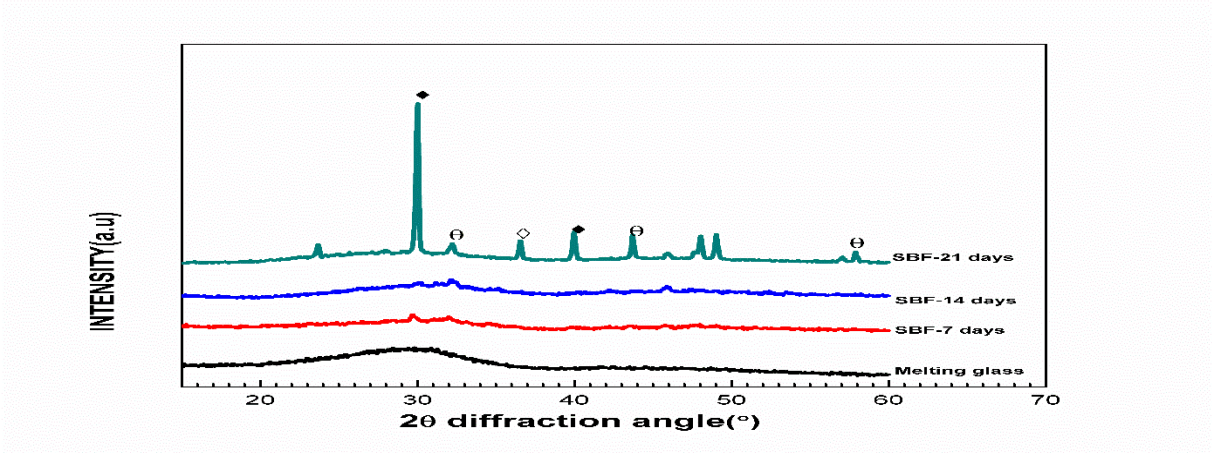

Figure4.8 X-ray pattern batch-2 glass powder SBF samples and their phases with reference code mention in table (4.3)

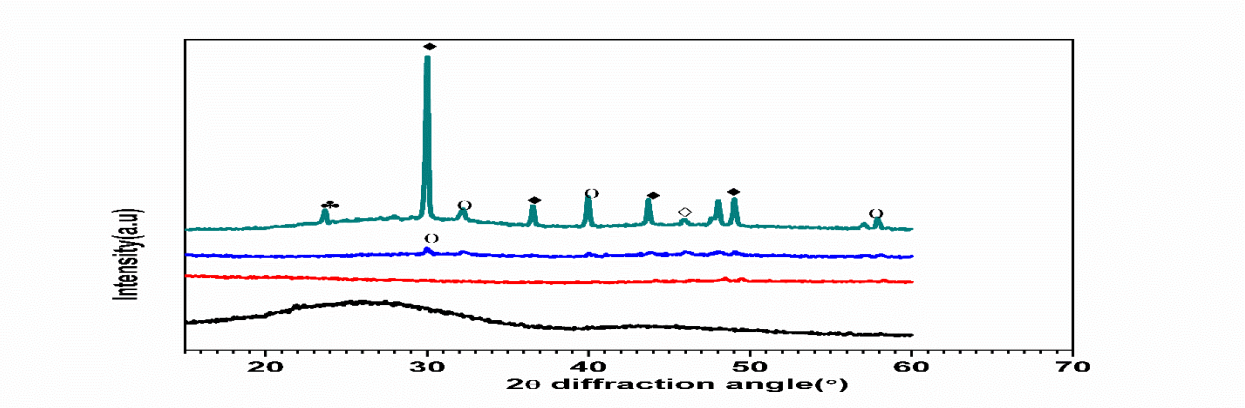

Figure4.9 X-ray pattern batch-3 glass powder SBF samples and their phases with reference code mention in table (4.3)

Symbols	Phases form	References
♦	β-Ca3 (PO4)2	09-0169
♣	CaPO3(OH)	09-0080
Θ	Ca5 (PO4)3 (OH)	73-1731
◊	BPO4	11-0272

Table (4.3) XRD analysis phases and reference code

From the above-given figures of the X-Rays Diffraction patterns of the different kinds of samples immersed in simulated body fluid for different days, after that taking out from the SBF and XRD analysis of the samples. The XRD analysis suggest that formation of calcium phosphate as primary phases with some other phases are present there, from this (09-0169) JCPDS reference pattern we conformed the formation of whitelokite (β-Ca3 (PO4)2) phase. The sample also tested using Invitro SBF study that revealed that hydroxyapatite layer gradually developed with increasing days of study.

4.3 DSC Analysis

4.3.1 DSC Analysis Batch-1

The glass transition temperature (Tg), crystallization temperature (Tp), and activation energy of the crystallization peaks value of all three heating rates batch-1 are shown in the table-4.4

Heating Rate	Tg (^{0}C)	1st peak Tp(^{0}C)	2nd Tp(^{0}C)
5k-min	675	747	839
10k-min	698	760	857
15k-min	704	769	870

Table 4.4 DSC parameters at different heating rates.batch-1

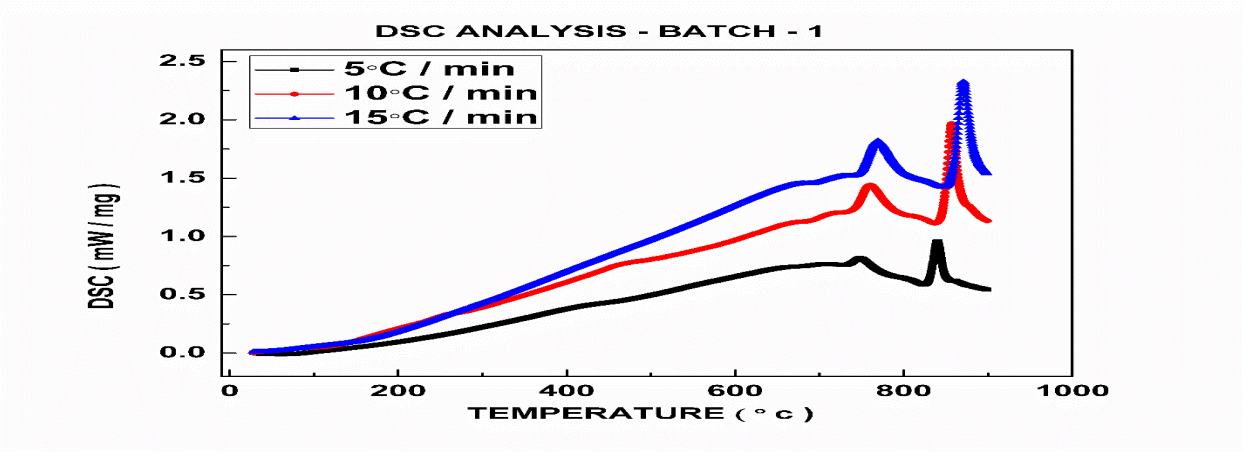

Fig 4.10 DSC-TG plot of the Batch-1 glass powder

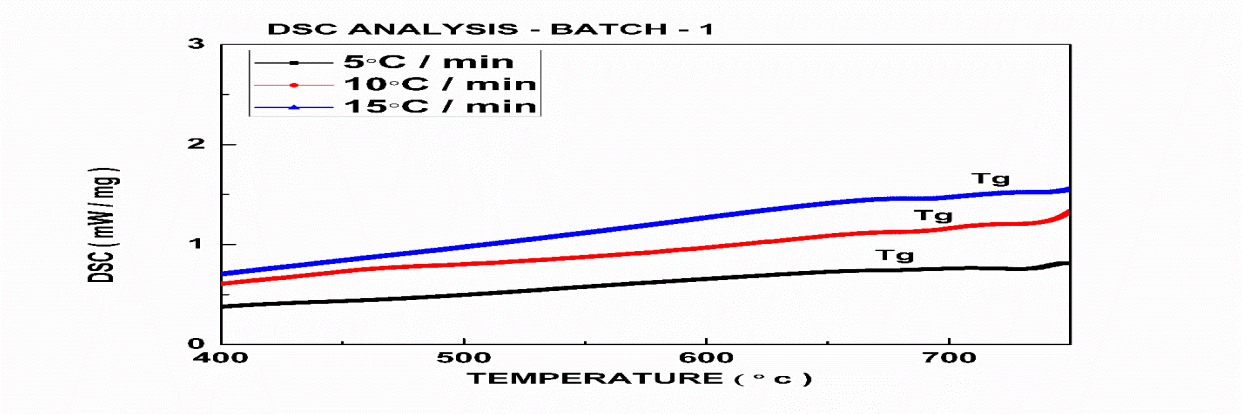

Figure 4.11 **Tg** different heating rates.batch-1

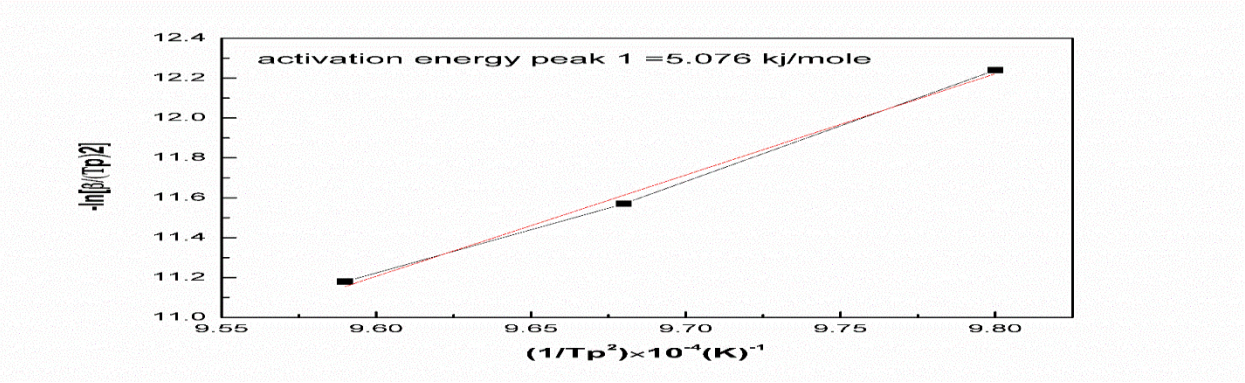

Figure-4.12.1 Activation Energy peak first

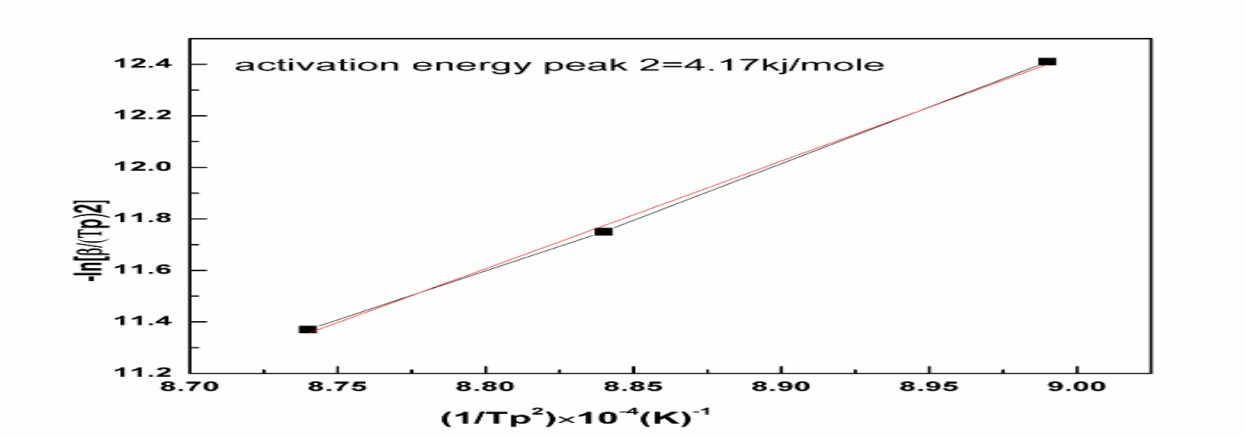

Figure-4.12.1 Activation Energy peak second

Figure 4.10 describe the DSC curves of the synthesize powder at different heating rates in the range 5 - 15◦C/min. In all three graphs two prominent exothermic peaks has been detected at 700–900 ◦C. Table (4.4) describe all temperature range for possible glass transition temperature and crystallization peaks. Figure 4.10 first exothermic peaks comes from the crystallization and second exothermic peaks come from the rearrangement of whitelokite phase. Figure 4.11 describes the glass transition temperature at three heating rates of batch-1 powder and cooled to room temperature, all the samples showed a glassy phase, with partial melting. From Kissinger question the plot shows $[-\ln(\alpha/T_p^2)]$ versus $1/T$p was presented in the figure - 4.12.1 the correlation parameter indicates a verygood fitting. The value of the activation energy for crystallization peaks calculated from the slope of the fig – 4.12.1 is 5.076 kJ/mol and 4.17 kJ/mol for 1st and 2nd peaks respectively, at different heating rates.

4.3.2 DSC Analysis Batch-2

The glass transition temperature (Tg), crystallization temperature (Tp), and activation energy of the crystallization peaks value of all three heating rates batch-2 are shown in the table (4.5)

Heating Rate	Tg (^{0}C)	1st peak Tp(^{0}C)	2nd Tp(^{0}C)
5k-min	671	747	843
10k-min	680	795	859
15k-min	687	763	873

Table 4.5 DSC parameters at different heating rates.batch-2

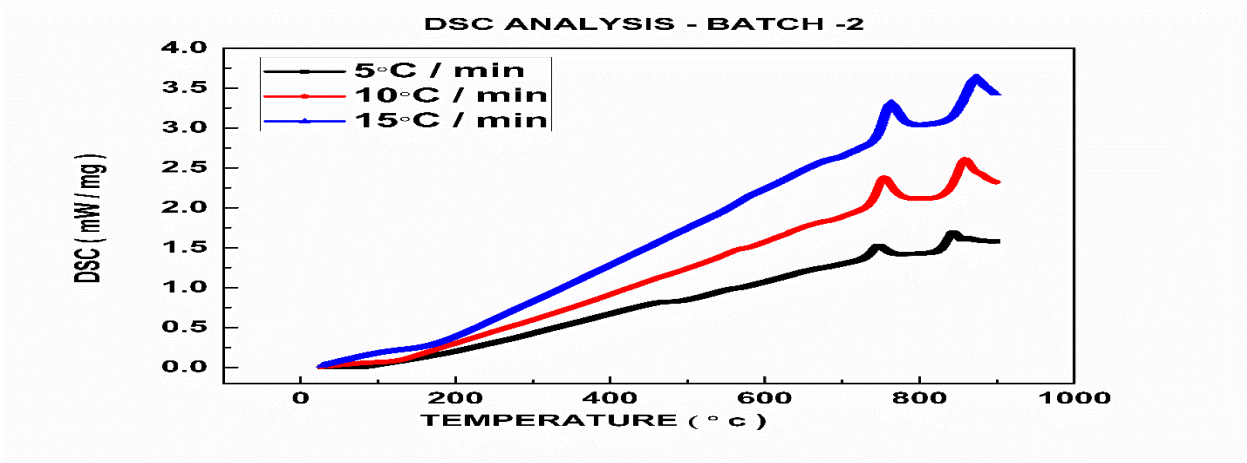

Fig 4.13 DSC plot of the Batch-2 glass powder

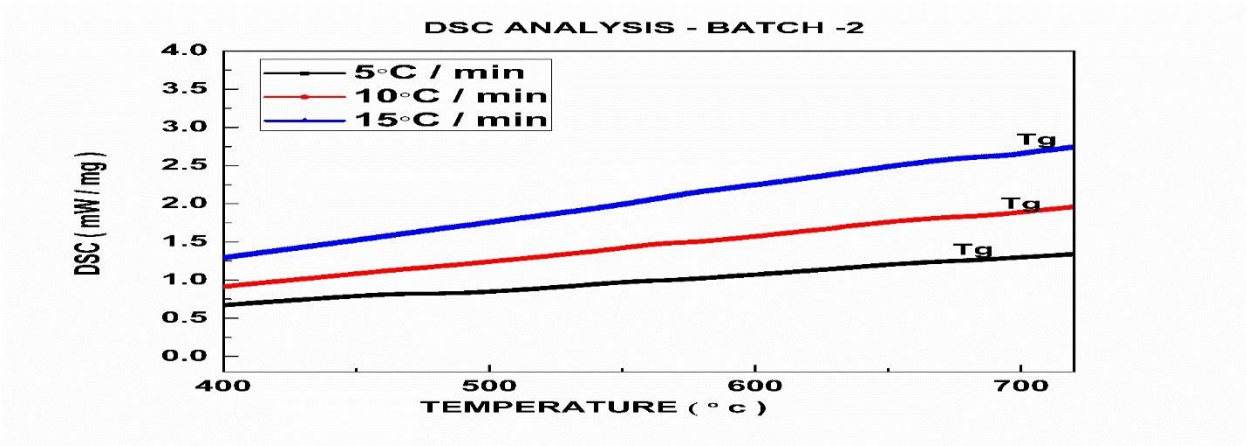

Figure 4.14 **Tg** different heating rates.batch-2 glass powder

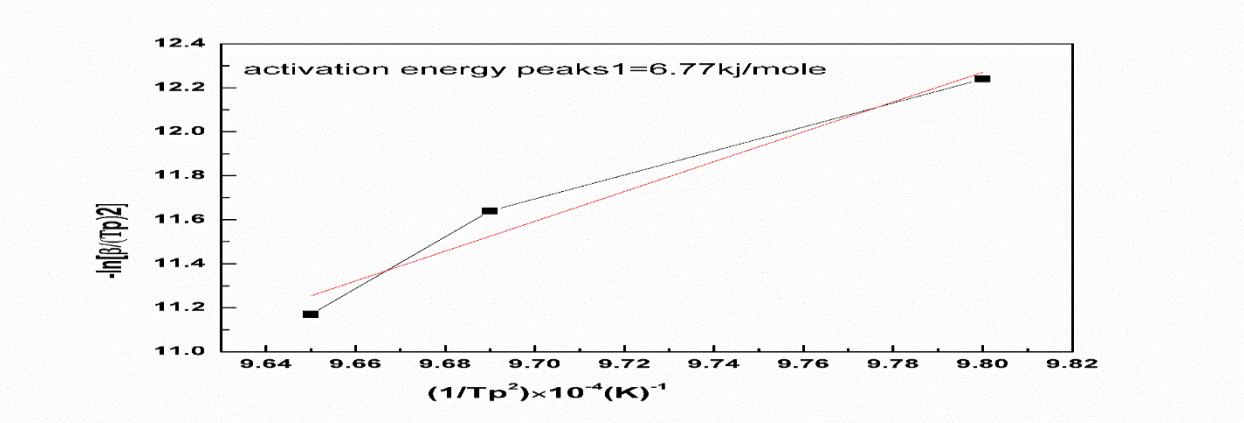

Figure-4.15.2 Activation Energy peak first batch-2

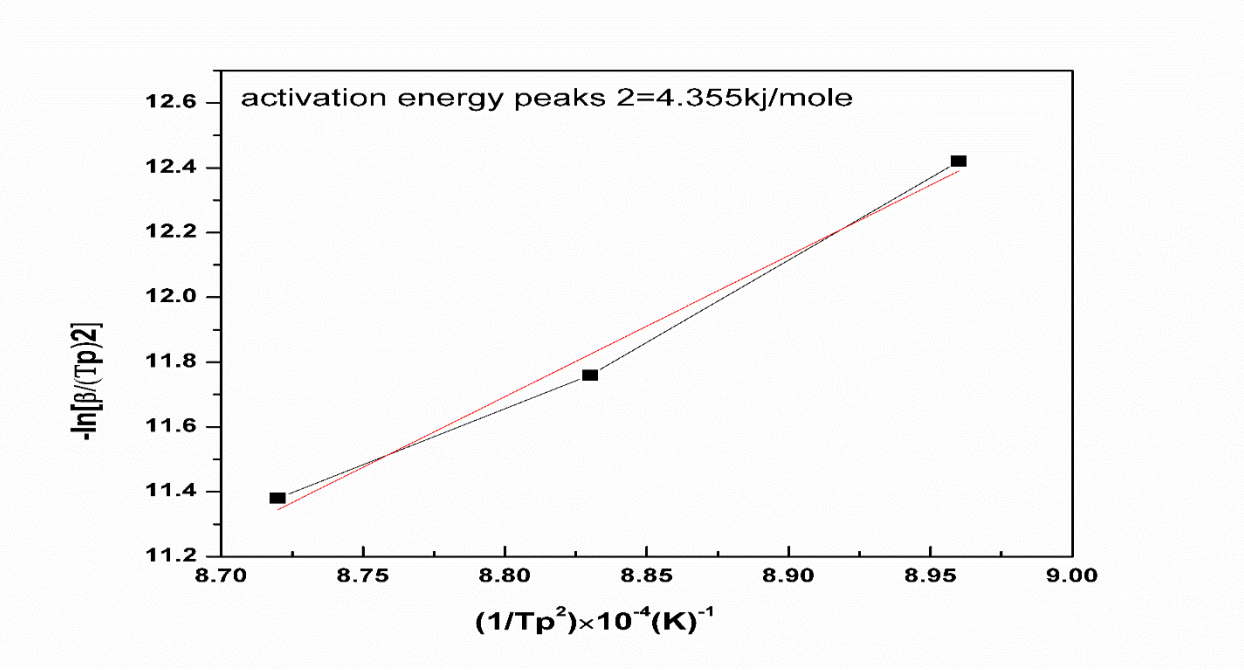

Figure-4.15.2 Activation Energy peak second batch-2

Figure 4.13 describe the DSC curves of the synthesize powder at different heating rates in the range 5 - 15◦C/min. In all three graphs two prominent exothermic peaks has been detected at 700–900◦C. Table (4.5) describe all temperature range for possible glass transition temperature and crystallization peaks. Figure 4.13 first exothermic peaks comes from the crystallization and second exothermic peaks come from the rearrangement of whitelokite phase. Figure 4.14 describes the glass transition temperature at three heating rates of batch-2 powder and cooled to room temperature, all the samples showed a glassy phase, with partial melting. From Kissinger question the plot of $[-\ln(\alpha/T_p^2)]$ versus $1/T$p presented in above figure (4.15.2) the correlation parameter indicates a very good fitting. The value of the activation energy for crystallization peaks calculated from the slope of the graphs are 5.076 kJ/mol and 4.17 kJ/mol for 1st and 2nd peak respectively.

4.3.3 DSC Analysis Batch-3

The glass transition temperature (Tg), crystallization temperature (Tp), and activation energy of the crystallization peaks value of all three heating rates batch-2 are shown in the table (4.6)

Heating Rate	**Tg (^{0}C)**	**1st peak Tp(^{0}C)**
5k-min	627	684
10k-min	641	693
15k-min	645	704

Table 4.6 DSC parameters at different heating rates.batch-3

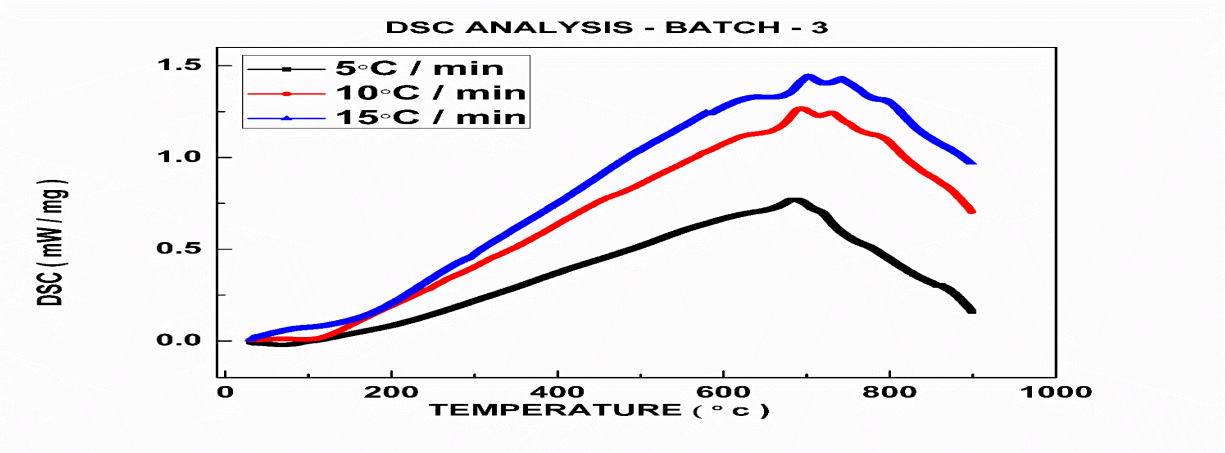

4.16 DSC plot of the Batch-3 glass powder

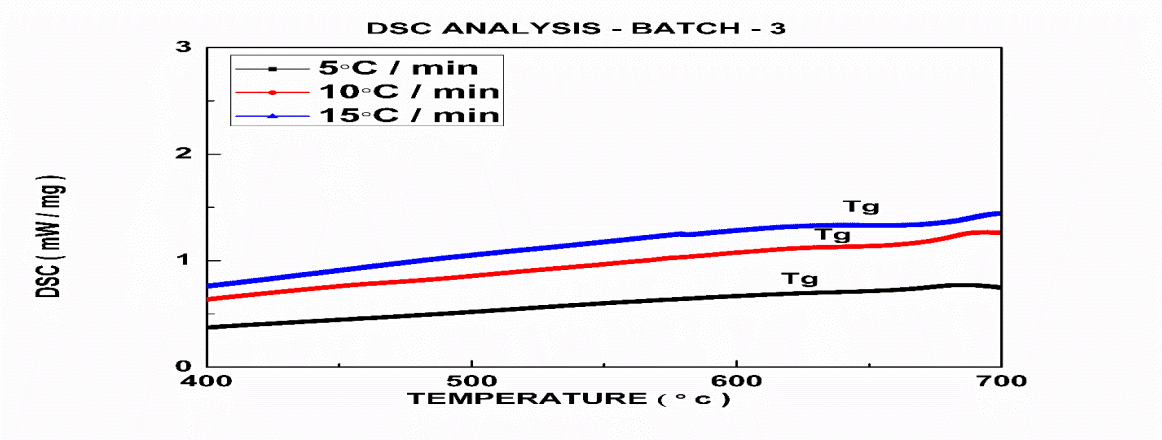

Figure 4.17 **Tg** different heating rates.batch-3 glass powder

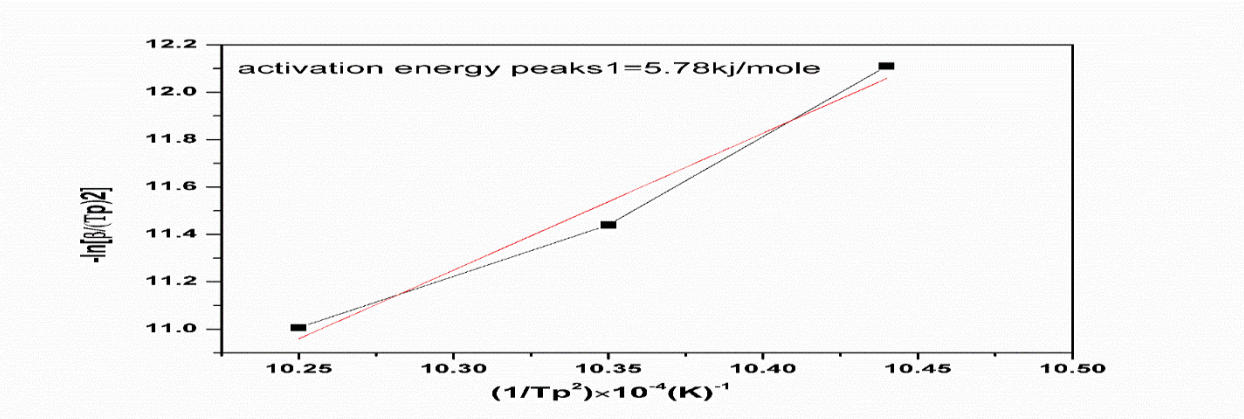

Figure-4.18 Activation Energy peak batch-3

Figure 4.16 describe the DSC curves of the synthesize powder at different heating rates in the range 5 - 15°C/min. In all three graphs two prominent exothermic peaks has been observed at 700–900°C. Table (4.6) describes the temperature range for possible glass transition and crystallization peaks. Figure 4.16 first exothermic peaks comes from the crystallization and rearrangement of whitelokite phase. Figure 4.17 describes the glass transition temperature at three heating rates of batch-3 powder and cooled to room temperature, all the samples showed a glassy phase, with partial melting. From Kissinger question the plot $[-\ln(\alpha/T_p^2)]$ versus $1/T_p$ showed in the above figure (4.15.2), the correlation parameter indicates a very good fitting. The value of the activation energy for crystallization peaks calculated from the slope of the graph were found to be 5.78 kJ/mol.

4.4 Dilatometry Analysis

The figure 4.19 shows the dilatometry study of batch-1, batch-2 and batch-3 at 10^0c/min heating rate. All three curves shows three distinct regions after glass transition temperature. The first slop indicates the densification of sample, and increases from batch 1-3 i.e., 6.42%, 13.76% and 19.77% this is due to increase in the amount of Ca/P molar ratio. which may be due to the diffusion of Ca^{2+} into the glass system. The second slop describe the crystallization of sample, this also increases with increasing amount of Ca/P Molar ratio. The third slop indicates the melting of the samples, Which also follows the same trend.

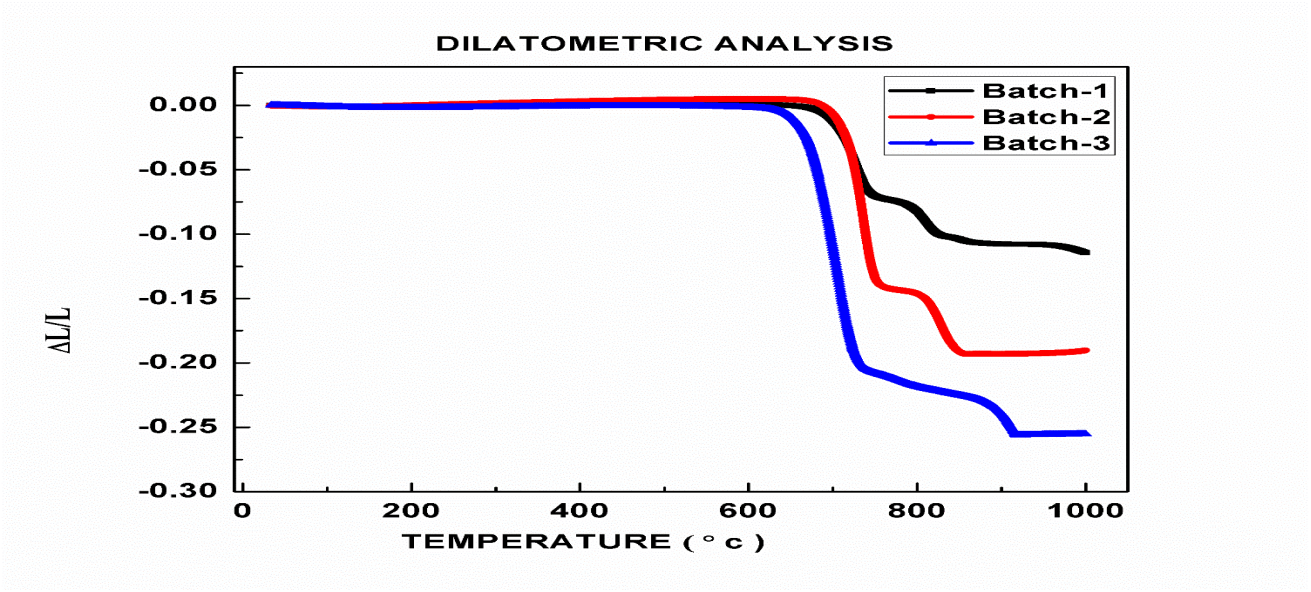

Fig 4.19: Dilatometry plot of Batch-1, Batch-2 and Batch-3 bioglass sample.

Sample	Tg(^{o}C)
Batch-1	698
Batch-2	680
Batch-3	641

Table -4.7 Glass transition temperature

4.5 Linear shrinkage Analysis

4.5.1 Linear Shrinkage Analysis of the dense samples

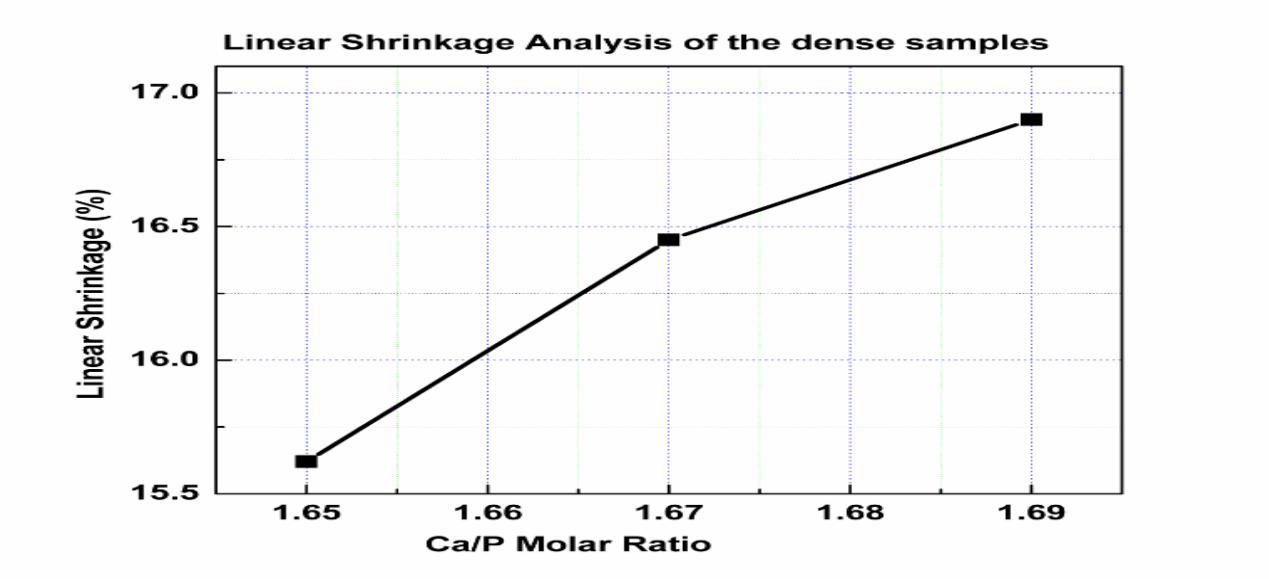

Figure 4.20 Linear Shrinkage of the dense samples

Sample	Linear Shrinkage (%)	Ca/P Molar Ratio
(0P)	15.62	1.65
(0P)	16.45	1.67
(0P)	16.9	1.69

Table 4.8 Linear Shrinkage of the dense samples

From the above figure 4.20 it was observed that the linear shrinkage increases with Ca/P molar ratio, which may be due to the diffusion of Ca^{2+} into the glass system resulting a better densification and at the same time the apparent porosity also decreased with increase molar ratio Ca/P.

4.5.2 Linear Shrinkage Analysis of the Pore former samples

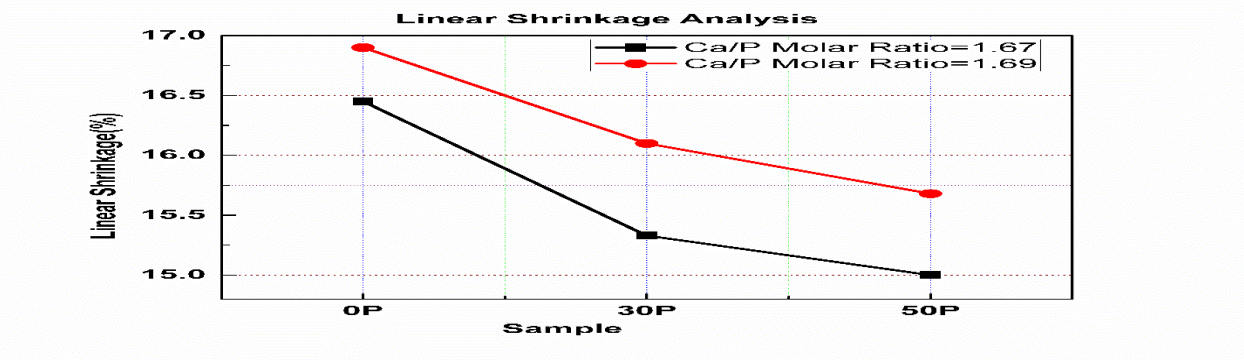

Figure 4.21 Linear Shrinkage of the pore former samples

Sample	Linear Shrinkage (%)	Linear Shrinkage (%)
	Ca/P Molar Ratio 1.67	Ca/P Molar Ratio 1.69
(0P)	16.45	16.90
(30P)	15.33	16.10
(50P)	15.00	15.68

Table 4.9 Linear Shrinkage of the pore former samples

From the above figure 4.21 it was observed that the linear shrinkage increased with the addition of pore former naphthalene for the samples with Ca/P ratio 1.67 and 1.69. The sample Ca/P -1.67 showed a lower shrinkage compared to the sample Ca/P 1.69 after addition of pore former naphthalene. From the above observation, it was clear that with an increase in the molar ratio results in a better linear shrinkage. Linear shrinkage decreases with an increase in naphthalene content, but the effect was not much prominent.

4.6 Bulk Density Analysis

4.6.1 Bulk density analysis of the dense samples

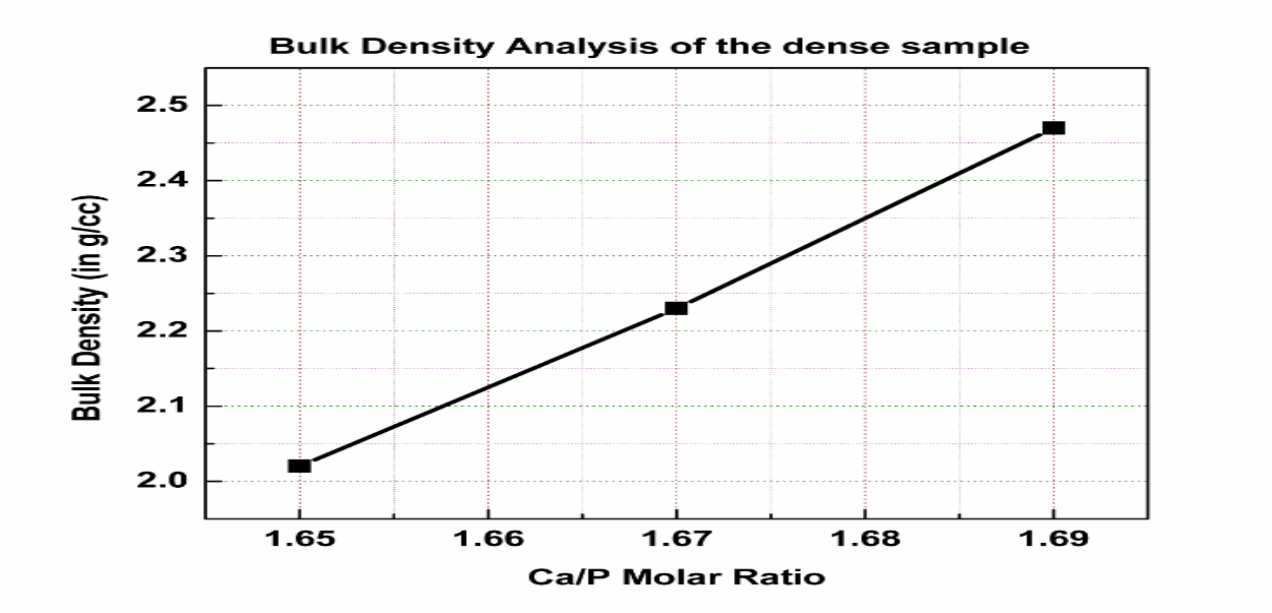

Figure 4.22 Bulk Density of the dense samples

Sample	Bulk Density (g/cc)	Ca/P Molar Ratio
(0P)	2.02	1.65
(0P)	2.23	1.67
(0P)	2.47	1.69

Table 4.10 Bulk Density of the dense samples

From the above figure 4.22 the bulk density value's of Ca/P = 1.65 to Ca/P = 1.69 are 2.02 to 2.47 respectively. From the above observation, it was clear that with an increase in the molar ratio results in a better densification, this is due to the higher amount of Ca2+ ions diffuse into the glass system.

4.6.2 Bulk density Analysis of the pore former samples

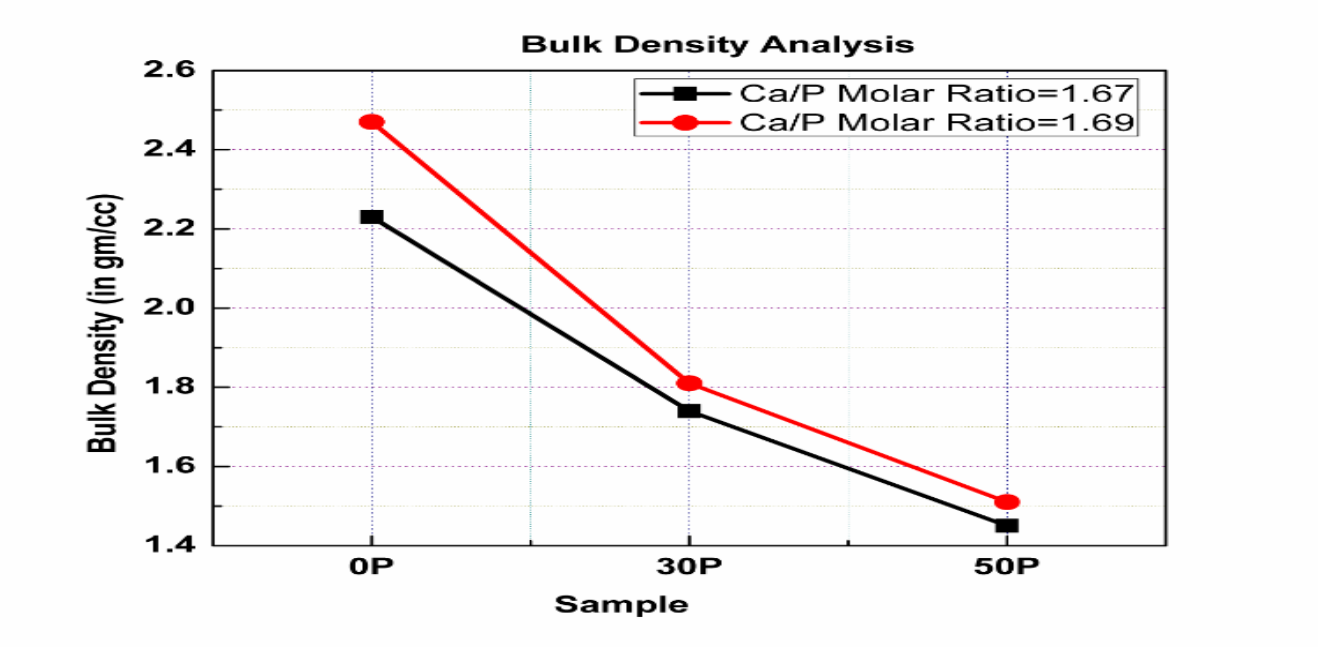

Figure 4.23 Bulk Density of the pore former sample

Sample	Bulk Density(g/cc)	Bulk Density(g/cc)
	Ca/P Molar Ratio 1.67	Ca/P Molar Ratio 1.69
(0P)	2.23	2.47
(30P)	1.74	1.81
(50P)	1.45	1.51

Table 4.11Bulk Density of the pore former samples

From the above figure 4.23 it was observed that there was a small increase in bulk density of the samples with an increase in Ca/P Molar ratios (1.67 to 1.69). It was observed that the bulk density of the samples decreased with increase in the weight percentage of the naphthalene.

4.7 Apparent Porosity Analysis

4.7.1 Apparent Porosity Analysis of the dense samples

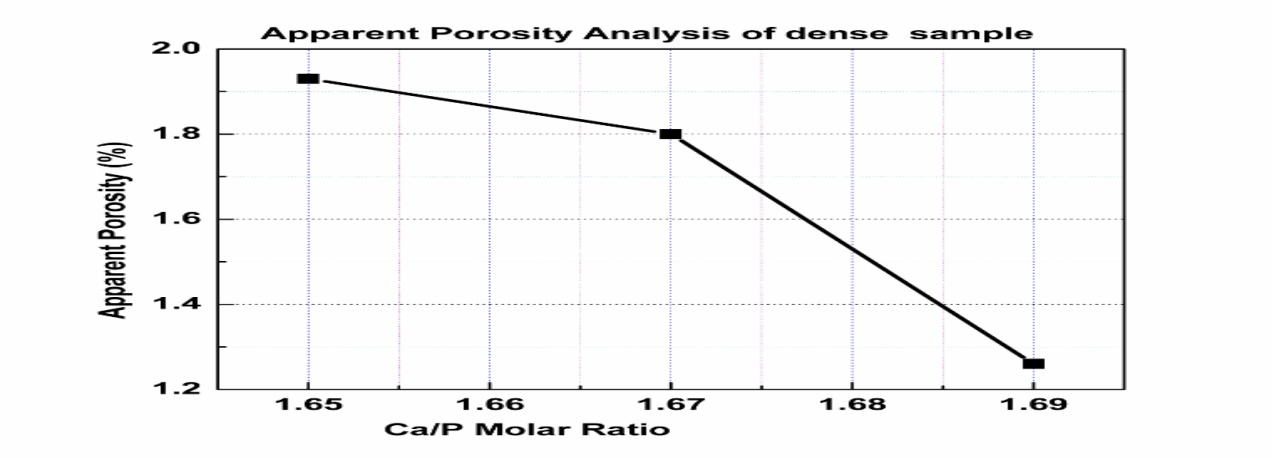

Figure 4.24 Apparent Porosity of the dense samples

Sample	Apparent Porosity (%)	Ca/P Molar Ratio
(0P)	1.93	1.65
(0P)	1.80	1.67
(0P)	1.26	1.69

Table 4.12 Apparent Porosity of the dense samples

From the above figure 4.24 it was observed that the decrement in the AP value is very small with the increase in Ca/P molar ratio. It was also observed that without pore former addition in the batch composition, the AP value's does not change significantly, thus resulting in dense samples.

4.7.2Apparent Porosity Analysis of the pore former samples

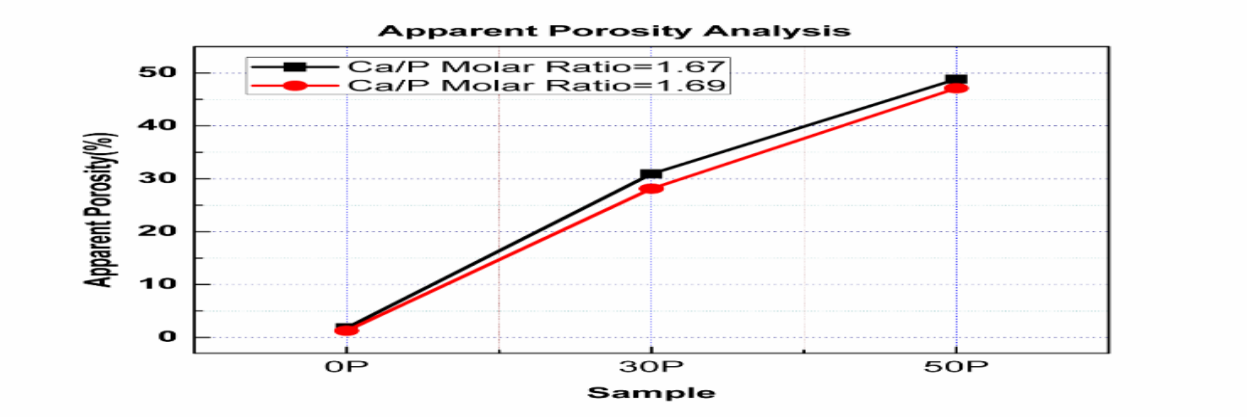

Figure 4.25 Apparent Porosity of the pore former samples

Sample	Apparent Porosity (%)	Apparent Porosity (%)
	Ca/P Molar Ratio 1.67	**Ca/P Molar Ratio 1.69**
(0P)	1.80	1.26
(30P)	30.91	28.11
(50P)	48.82	47.10

Table 4.13 Apparent porosity of the pore former samples

From the figure 4.25 it can be observed that the apparent porosity decreased with the increase in Ca/P Molar ratio (1.67 to 1.69) in glass batch composition. It was also observed that the marked increase in the AP values with the increase in a weight percentage of naphthalene used. So, we may also conclude that the porosity as high as 50 percentage can be achieved by using naphthalene as a pore former.

4.8 Diametral tensile strength measurement

4.8.1 Diametral tensile strength of dense samples

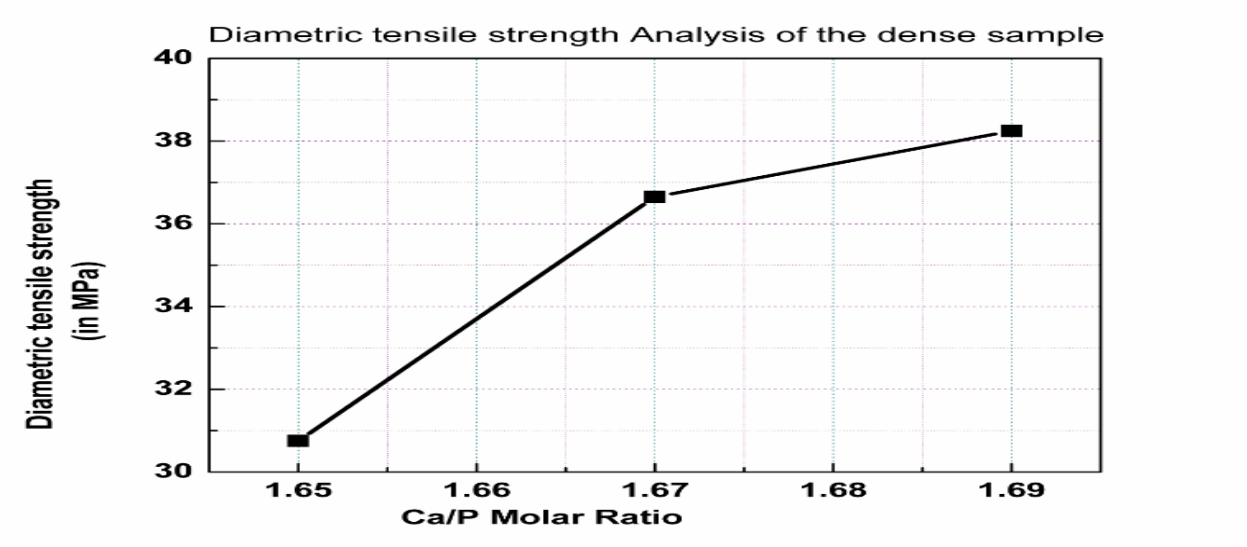

Figure 4.26 Diametral tensile strength of the dense samples

Sample	Diametral tensile strength (in MPa)	Ca/P Molar Ratio
(0P)	30.75	1.65
(0P)	36.65	1.67
(0P)	38.24	1.69

Table4.14 Diametral tensile strength of the dense samples

From the above figure 4.26 the diametral tensile strength value shows a real improvement, with an increase in Ca/P Molar ratio (1.65 to 1.69).

4.8.1 Diametral tensile strength analysis of the pore former samples

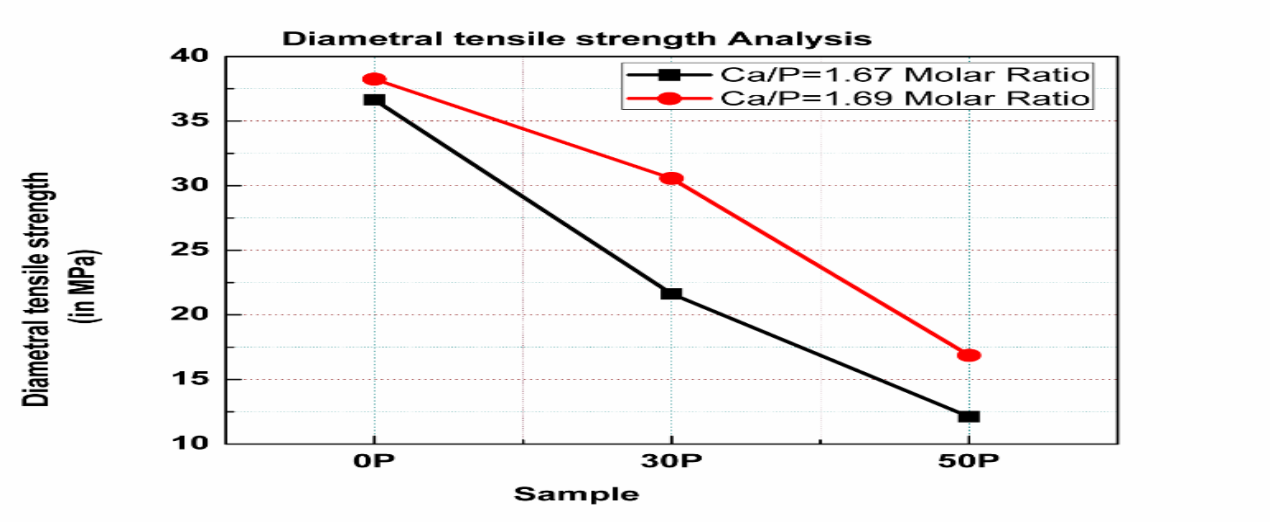

Figure 4.27 Diametral tensile strength of the pore former samples

Sample	Diametral tensile strength (in MPa)	Diametral tensile strength (in MPa)
	Ca/P Molar Ratio 1.67	**Ca/P Molar Ratio 1.69**
(0P)	36.65	38.24
(30P)	21.62	30.56
(50P)	12.11	16.86

Table 4.15 Diametral tensile strength of the pore former samples

From the above figure 4.27 the diametral tensile strength value showed an significant improvement with an increase in Ca/P Molar ratio (1.67 to 1.69) in batch composition. Except in the case of the 50 percentage naphthalene containing glass samples, where not much improvement could be observed. The diametral tensile strength value decreased with increase in

the weight percentage of the naphthalene. With the naphthalene size between 150 to 200 micron. The maximum diametral tensile strength value was found to be 38.24 MPa for 0% pore former (Ca/P Molar ratio (1.69)) and minimum 12.11 MPa for 50% pore former (Ca/P Molar ratio(1.67)).

4.9 Three-point bending movement measurement

4.9.1 Three-point bending movement of the dense samples

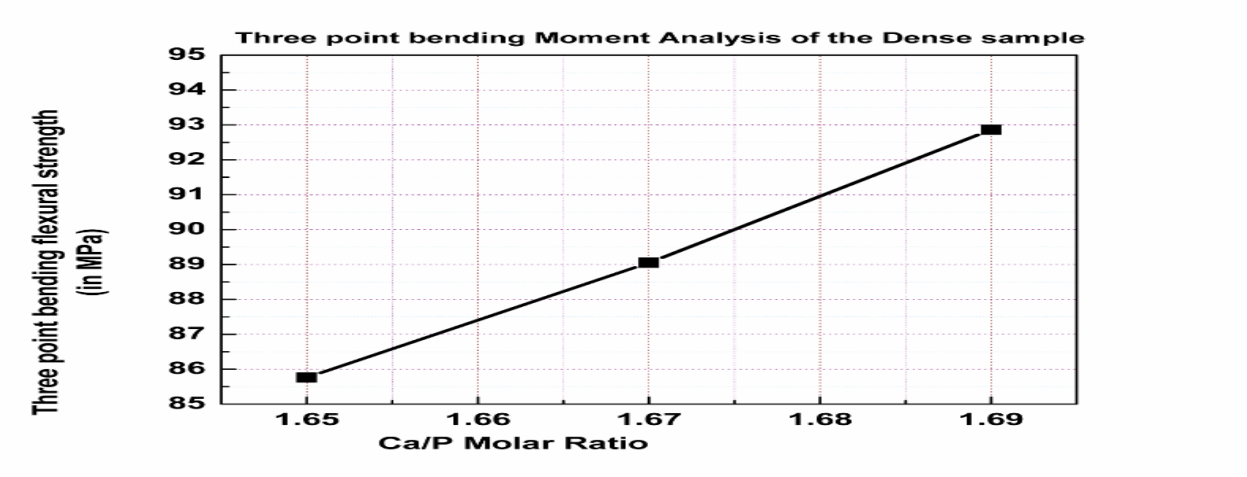

Figure 4.28 Three points bending moment of the dense samples

Sample	Three-point bending flextural strength (in MPa)	Ca/P Molar Ratio
(0P)	85.76	1.65
(0P)	89.05	1.67
(0P)	92.86	1.69

Table 4.16 Three point bending moment of the dense samples

From the above figure 4.28 it was observed that the three-point bending flextural strength increases with increase in Ca/P molar ratios (1.65, 1.68 and 1.69). The maximum flextural

strength was found to be 92.86 MPa for the sample with Ca/P Molar ratio 1.69 and minimum was 8576 MPa for the sample with Ca/P molar ratio 1.65.

4.9.1 Three-point bending moment of the pore former samples

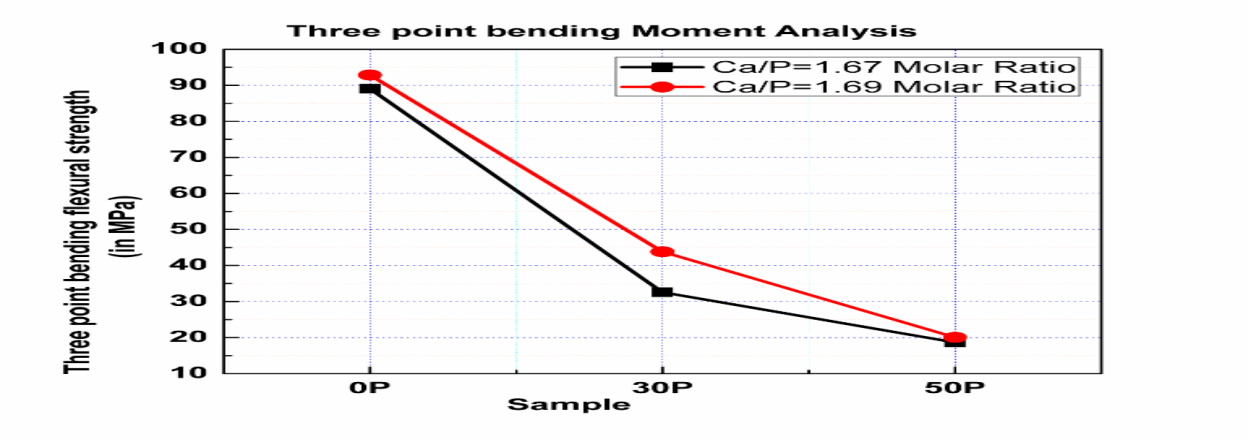

Figure 4.29 Three points bending moment of the pore former samples

Sample	Three-point bending flextural strength (in MPa)	Three-point bending flextural strength (in MPa)
	Ca/P Molar Ratio 1.67	**Ca/P Molar Ratio 1.69**
(0P)	89.05	92.86
(30P)	32.56	43.81
(50P)	18.65	20.06

Table 4.17 Three points bending moment of the pore former samples

From the above figure 4.29 three-point bending flextural strength value showed a great improvement with increase in Ca/P molar ratio. Except in the case of the 50 weight percentage of

the naphthalene containing samples, where much improvement could be not seen. The flextural value decreases with increase in the weight percentage of naphthalene (150 to 200 micron size). The maximum flextural strength was 92.86 MPa for zero pore former samples with Ca/P molar ratio 1.69 and minimum was 18.65MPa for 50 percentage pore formers sample with Ca/P Molar ratio 1.67.

4.10 Vickers hardness measurement of dense sintered samples

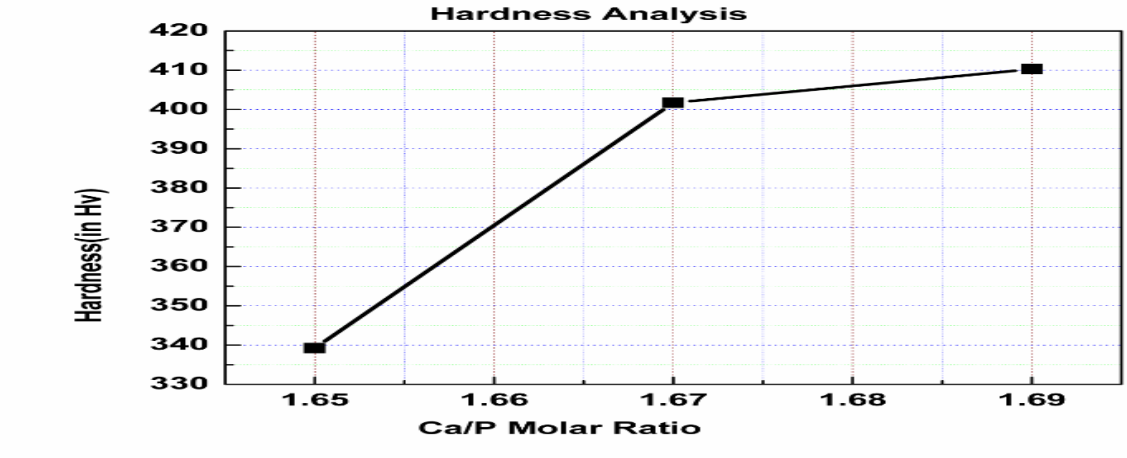

Figure 4.30 Vickers hardness of the dense samples

Samples Name	D_1 (In µm)	D_2 (In µm)	Hardness (in Hv)	Ca/P Molar Ratio
(0P)	117	119	339.2	1.65
(0P)	118	119.1	401.7	1.67
(0P)	115.8	116.4	410.3	1.69

Table 4.18 Vickers hardness of the dense samples

From the above figure 4.30 the Vickers hardness of the zero pore former (dense) samples increased with increase the Ca/P molar ratio. The maximum Vickers hardness 410.4 Hv for zero

poreformer glass samples prepare with Ca/p 1.69 Molar ratio and minimum for 339.2Hv for zero pore glass samples prepared with Ca/P 1.65 Molar ratio.

4.11 Scanning Electron microscopy

21 days SBF Dense samples images

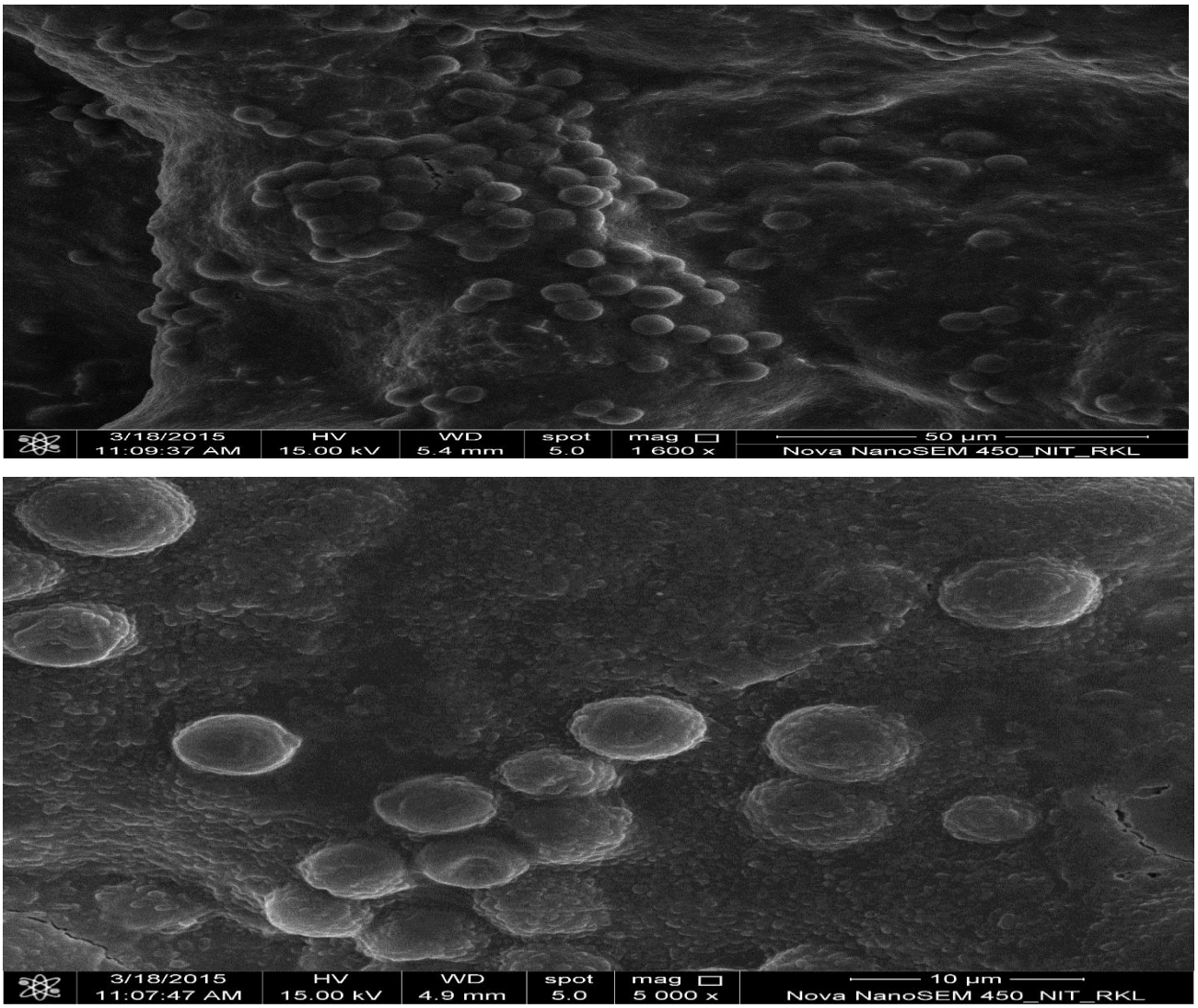

Figure 4.31 21 days SBF FESEM Images of Batch-2 & 3

21 days SBF porous samples images

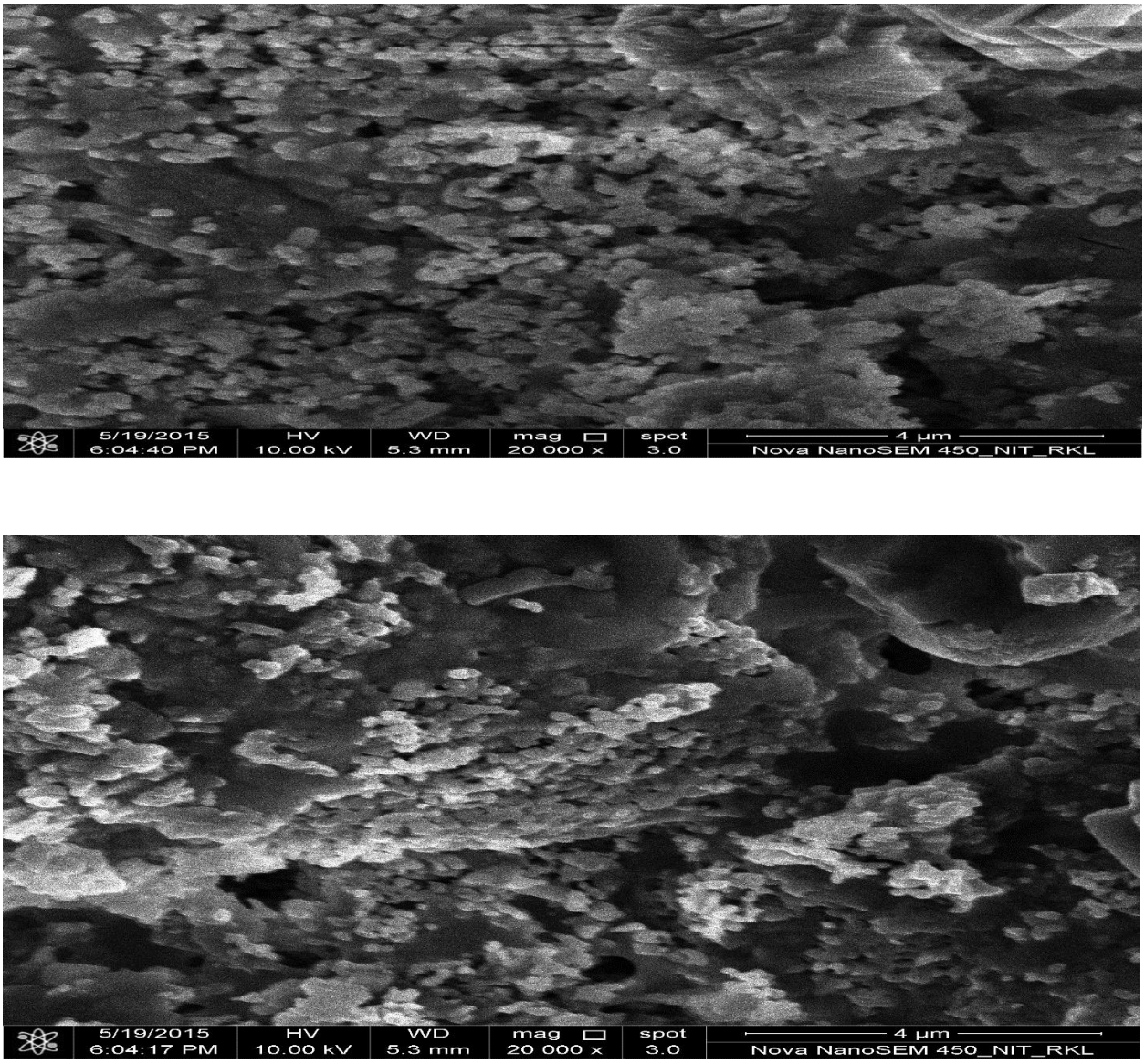

Figure 4.31 21 days SBF FESEM Images of Batch – 2 & 3

From above FESEM images, it was clear that the formation of an amorphous layer, which results from the deposition of amorphous hydroxyapatite. After 21 days of observation they suggest that the samples are not only biocompatible but also bioactive in nature.

Conclusions:

The glass has been prepared in system 20 it.%[B_2O_3]-80wt%[CaO-P_2O_5] With varying Ca/P Molar ratios (1.65, 1.67 & 1.69) by melt quenching method. XRD analysis of this powder confirmed the powder is amorphous in nature. DSC Analysis reviled that samples were thermally stable up to 700^0C and crystallization temperature of different sample increases with varying Ca/P Molar ratio. This is because of rearrangement of phosphate phase (whitelokite). Dilatometry data explainss higher amount Ca/P ratio subsequently affect the bulk density of the glass samples. Thermal stability has been confirmed by DSC & TG analysis. DTS, flexural strength and Vickers hardness has been done to check the mechanical behavior of the glasses. Mechanical properties increased with increase in Ca/P ratio. Invitro bioactivity has been done by immersing the glass samples in SBF for 2 weeks and showed a carbonated hydroxy appetite layer formation with increasing the days of study, which suggest the glasses are not only bio compatible also bio active in nature. All results suggest that this glasses can be used as a filler material in orthopedic surgery and medical applications.

References

[1.] L.L. Hench, R.J. Splinter W.C. Allen, T.K. Greenlee Jr. Bonding mechanism at the interface of ceramics prosthetic materials. J Biomed Mater Res Symp 2(1971) 117–41

[2]. T.Kokubo , Shigematsu M, Nagashima Y, Tashiro M, Nakamura T,Yamamuro T, et al. Apatite- and wollastonite-containing glass ceramics for prosthetic application. Bull Inst Chem Res Kyoto Univ. 60(1982) 260–68..

[3] S.F. Hulbert. The use of alumina and zirconia in surgical implants. In:Hench LL, Wilson J, editors. An introduction to bioceramics. Singapore: World Scientific; (1993) 25–40.

[4] J. M.archo, J.L Kay, Gumaer RH, Drobeck HP. Tissue, cellular and subcellular events at bone-ceramic hydroxyapatite interface. J Bioeng 1(1977)79–92.

[5] L.L. Hench Bioceramics: from concept to clinic. J Am Ceram Soc 74(1991)1487–510.

[6]. M. Neo, T .Nakamura, C. Ohtsuki,T. Kokubo ,T.Yamamuro . Apatite formation on three kinds of bioactive material at an early stage in vivo: a comparative study by transmission electron microscopy. JBiomed Mater Res 27(1993) 999–1006.

[7]. T. Kokubo A/W glass-ceramic: processing and properties. In: Hench LL, Wilson J, editors. An introduction to bioceramics. Singapore:World Scientific; (1993) 75–88.

[8]. S.D. Stookey, Ind. Eng. Chem. 51 (1959) 805.

[9]. W. Vogel, Chemistry of Glass, American Ceramic Society, Columbus, OH,(1985)

[10] R.K. Brow, D.R. Tallant, J. Non-Cryst. Solids 222 (1997) 396.

[11] L. Koudelka, P. Mosˇner, Mater. Lett. 42 (2000) 194.

[12] L.L. Hench, J. Am Ceram Soc 74 (1991) 1487.

[13] HenchLL. Bioceramics. J Am Ceram Soc 1998;81(7):1705–28.

[14] Rey C. Calcium phosphate biomaterials and bone mineral. Differences in composition, structures and properties. Biomaterials
1990;11(BIMAT 89):13–5.

[15] Ducheyne P, Qiu Q. Bioactive ceramics: the effect of surface reactivity on bone formation and bone cell function. Biomaterials 1999;20:2287–303.

[16] Ravaglioli A, Krajewski A. Bioceramics: materials, properties, application. London: Chapman & Hall; 1992. p. 156–197.

[17]J.R. Jones, Lisa M. Ehrenfried&L.L.Hench, Biomaterials 27 (2006) 964–973.

[18]K. Rezwan, Q.Z. Chen, J.J. Blaker& Aldo Roberto Boccaccini, Biomaterials 27 (2006) 3413–3431

[19]Marivalda M. Pereira, Arthur E. Clark and Larry L. Hench, J Am Ceram Soc. 1995;78(9):2463–8

[20] L.L.Hench, J Mater Sci: Mater Med (2006) 17:967–978

[21]L.L.Hench, R. J. Splinter, T. K. Greenlee &W.C.Allen, J. Biomed. Mater. Res.(1971) 117

[22]L.L.Hench, A. E. Clark Jr & and H.F.Schaake, Int.J. Non-Cryst. Sol. 8–10, **(**1972)837

[23] J.R.Jones, ActaBiomaterialia 9 (2013) 4457–4486

[24] A.L.Girot, F.Z.Mezahi et al, Journal of Non-Crystalline Solids 357 (2011) 3322–3327